Supporting Information for

Straightforward supramolecular purification of C84 from fullerene extract

Ernest Ubasart,[a] Cristina García-Simón,[a] Míriam Pujals,[a] Karam Asad,[b] Nikos Chronakis,[b] Teodor Parella,[c] Xavi Ribas[a,*]

Table of Contents

1. Supplementary Methods

1.1. Materials and Instrumentation

Reagents and solvents were purchased from commercial sources and used without further purification unless otherwise stated. NMR data were collected on a Bruker 400 MHz AVANCE spectrometer in $CDCl_3$ or CD_3CN, and calibrated relative to the residual protons of the solvent. ESI-MS measurements were performed on a Bruker MicroTOF-Q-II using $CDCl_3$ or CH_3CN as a mobile phase. HPLC analysis of fullerenes was performed on an Agilent series 1200 chromatograph equipped with a Cosmosil Buckyprep-M column, or on a LC-9130 NEXT apparatus (Japan Analytical Industry Co.Ltd.) with monitoring at 320 nm and using toluene as an eluent at a flow rate of 0.5 ml/min. MALDI-TOF measurements were performed on a Bruker Daltonics Autoflex maX using DCTB and NaTFA as matrix. UV-Vis spectra were recorded on an Agilent 8452 UV-Vis spectrophotometer using a 1 cm quartz cell and CH_3CN as a solvent. Fullerene extract (70% C_{60}, 28% C_{70} and 2% higher fullerenes) was purchased from SES Research and used as received. Azafullerene $(C_{59}N)_2$ and nanocapsules **6**·$(BArF)_8$ and **7**·$(BArF)_8$ were prepared according to reported procedures.[1-3]

1.2. Synthesis and characterization of dialdehyde (ppp)

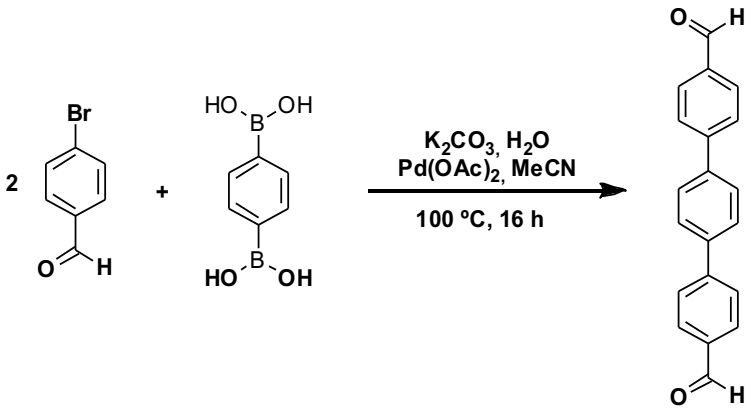

Supplementary Figure 1. Synthesis of (1,1':4',1''-terphenyl)-4,4''-dicarbaldehyde (ppp).

(1,1':4',1''-terphenyl)-4,4''-dicarbaldehyde (ppp) was synthetized following reported procedures.[4] 4-Bromobenzaldehyde (2.0 g, 1 mmol) was added in a 100 ml round-bottom flask. Benzene-1,4-diboronic acid (0.9 g, 0.6 mmol) dissolved in 16 ml of acetonitrile was

then added followed by the addition of K_2CO_3 (1.8 g, 2.4 mmol) dissolved in 26 ml of milliQ water. Finally, $Pd(OAC)_2$ (0.12 g, 0.1 mmol) was added and the reaction mixture was heated at 110 ºC for 16 h. After this time, 50 ml of water were added and the product was extracted with dichloromethane (3 x 20 ml). The organic phases were combined, dried over anhydrous $MgSO_4$ and filtered. The remaining solution was dried under vacuum and the product was obtained as a pale-yellow solid. (Yield: 80%).

^{1}H-NMR (400 MHz, $CDCl_3$) δ ppm: 10.08 (s, 2H, -CH), 7.99 (d, J=8.4 Hz, 4H, arom), 7.82 (d, J=8.2 Hz, 4H, arom), 7.77 (s, 4H, arom).

^{13}C-NMR (100 MHz, $CDCl_3$) δ ppm: 191.97 (C=O), 146.42 (C arom), 139.94 (C arom), 135.63 (C arom), 130.53 (CH arom), 128.15 (CH arom), 127.78 (CH arom).

HRMS (*m/z*): calculated 309.0889, found 309.0886 for ({diarylalkyne-ppp + Na}$^{+1}$); calculated 327.0998, found 327.0992 for ({diarylalkyne-ppp + H_2O + Na}$^{+1}$), calculated 341.1154, found 341.1148 for ({diarylalkyne-ppp + CH_3OH + Na}$^{+1}$).

1.3. Synthesis and characterization of S_2ppp

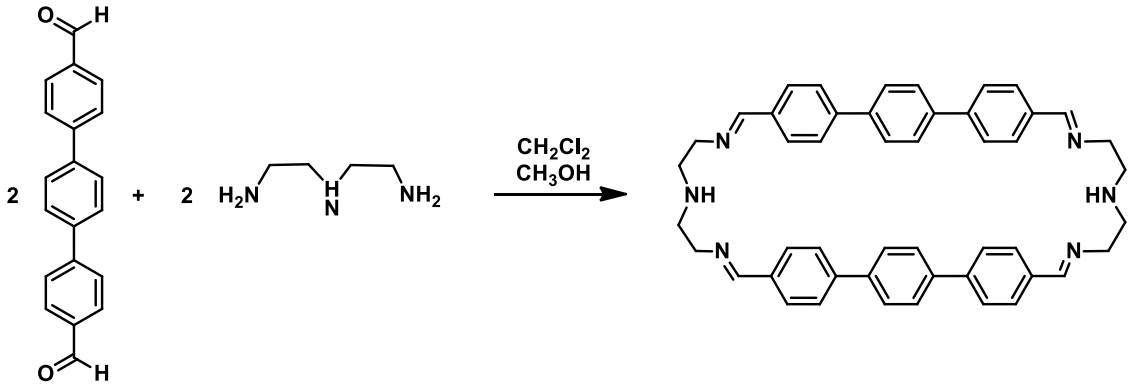

Supplementary Figure 2. Synthesis of the S_2ppp macrocycle.

(1,1':4',1''-terphenyl)-4,4''-dicarbaldehyde (0.78 g, 1 mmol) was dissolved in 250 ml of DCM and charged in a 250 ml addition funnel. Then, 294 µl (1 mmol) of diethylenetriamine were added in a 500 ml round-bottom flask containing 250 ml of MeOH. The dialdehyde solution was added dropwise into the amine solution during a period of 6 h and stirred for 16 h. After this time, a white solid was obtained.

^{1}H-NMR (400 MHz, $CDCl_3$) δ ppm: 8.35 (s, 4H, arom), 7.60 (d, J=8.3 Hz, 8H, arom), 7.49 (s, 8H, arom), 7.47 (d, J=8.3 Hz, 8H, arom), 3.84-3.82 (m, 8H, CH_2), 3.04-3.02 (m, 8H, CH_2).

^{13}C-NMR (100 MHz, $CDCl_3$) δ ppm: 162.03 (C sp^2 imine), 142.31 (C arom), 139.45 (C arom), 135.21 (C arom), 128.73 (CH arom), 127.54 (CH arom), 126.99 (CH arom), 60.14 (-CH_2-), 48.68 (-CH_2-).

HRMS (*m/z*): calculated 354.1965, found 354.1975 for ({S_2ppp + H}$^{+2}$); calculated 707.3857, found 707.3868 for ({S_2ppp + H}$^{+1}$).

1.4. Synthesis and characterization of H_2ppp

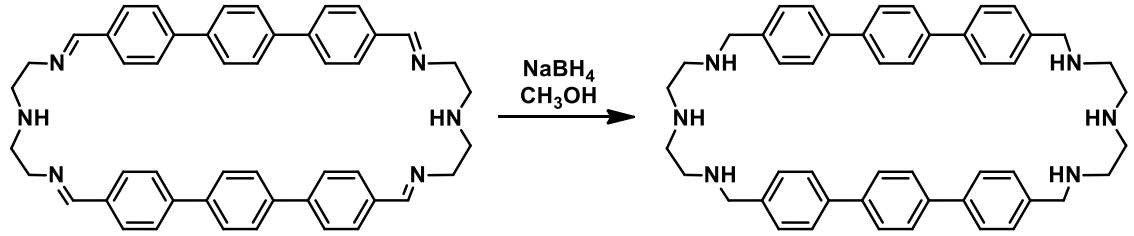

Supplementary Figure 3. Synthesis of H_2ppp.

0.52 g of $NaBH_4$ (10 mmols) were added into a S_2ppp solution in methanol and the reaction mixture was stirred for 16 h. After this time, 20 ml of an acid solution (HCl:H_2O 1:10) were added and the crude reaction mixture was stirred for 45 minutes. Then, the solution was evaporated under reduced pressure until a constant volume and 100 ml of H_2O were added. The product was extracted with $CHCl_3$ (3 x 50 ml) and the organic phases were combined, dried over anhydrous $MgSO_4$ and filtered. The remaining solution was dried under vacuum to afford the product as a white solid. (Yield: 87%).

^{1}H-NMR (400 MHz, $CDCl_3$) δ ppm: 7.54 (s, 8H, arom), 7.51 (d, J=8.2 Hz, 8H, arom), 7.37 (d, J=8.2 Hz, 8H, arom), 3.84 (s, 8H, CH_2), 2.93-2.85 (m, 16H, CH_2).

^{13}C-NMR (100 MHz, $CDCl_3$) δ ppm: 139.81 (C arom), 139.64 (C arom), 139.21 (C arom), 128.66 (CH arom), 127.40 (CH arom), 127.02 (CH arom), 53.70 (-CH_2-), 49.05 (-CH_2-), 48.38 (-CH_2-).

HRMS (*m/z*): calculated 358.2278, found 358.2281 for ({H_2ppp + H}$^{+2}$); calculated 715.4483, found 715.4493 for ({H_2ppp + H}$^{+1}$).

1.5. Synthesis and characterization of Me_2ppp

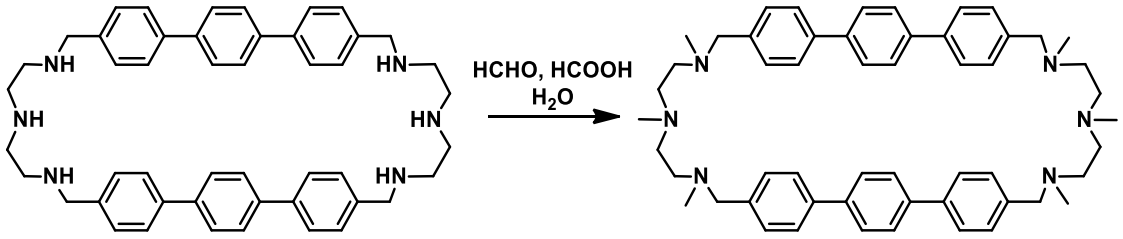

Supplementary Figure 4. Synthesis of the macrocyclic ligand, Me_2ppp.

0.97 g of H_2ppp (1 mmol) were added to a 100 ml round-bottom flask and mixed with 12 ml of formaldehyde, 10 ml of formic acid and 20 ml of water. The resulting mixture was heated at reflux for a period of 16 h. After this time, the reaction mixture was cooled to room temperature and the solvent was removed under reduced pressure. Then, 50 ml of NaOH 1M were added and the product was extracted with $CHCl_3$ (3 x 25 ml). The organic phases were combined, dried over anhydrous $MgSO_4$ and filtered. The remaining solution was dried under vacuum and the product was purified by recrystallization with acetone. (Yield: 80%).

^{1}H-NMR (400 MHz, $CDCl_3$) δ ppm: 7.48 (s, 8H, arom), 7.46 (d, J=8.2 Hz, 8H, arom), 7.32 (d, J=8.2 Hz, 8H, arom), 3.51 (s, 8H, CH_2), 2.59-2.53 (m, 16H, CH_2), 2.31 (s, 6H, CH_3), 2.24 (s, 12H, CH_3).

^{13}C-NMR (100 MHz, $CDCl_3$) δ ppm: 139.57 (C arom), 139.28 (C arom), 138.25 (C arom), 129.68 (CH arom), 127.33 (CH arom), 126.82 (CH arom), 62.31 (-CH_2-), 54.76 (-CH_2-), 54.56 (-CH_2-), 43.75 (-CH_3), 43.05 (-CH_3).

HRMS (*m/z*): calculated 400.2747, found 400.2741 for ({Me_2ppp + H}$^{+2}$); calculated 799.5422, found 799.5421 for ({Me_2ppp + H}$^{+1}$).

1.6. Synthesis and characterization of dinuclear Pd^{II} molecular clip $[Pd_2(Me_2ppp)(AcO)_2](OTf)_2$

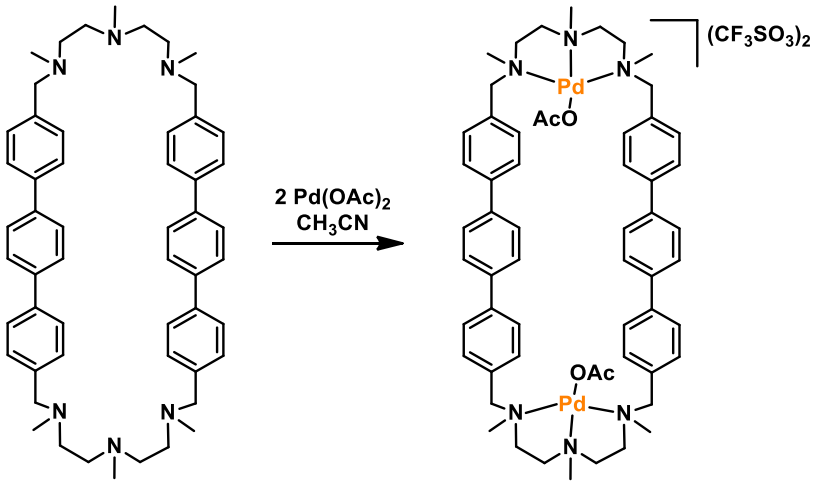

Supplementary Figure 5. Synthesis of $[Pd_2(Me_2ppp)(AcO)_2](OTf)_2$.

In a 250 ml round-bottom flask, 0.172 g of Me_2ppp (1 mmol), 0.101 g of $Pd(AcO)_2$ (2.1 mmols) and 85 ml of anhydrous CH_3CN were mixed. The mixture was heated at reflux under a nitrogen atmosphere for 16h. After this time, the reaction mixture was cooled to room temperature. Subsequently, an excess of CF_3SO_3Na salt was added (4.2 mmols)

and the mixture was stirred vigorously for 8h. The mixture was concentrated to the half of the volume under reduced pressure, filtered through Celite and recrystallized by slow diffusion of diethyl ether. The product was obtained as a yellow crystalline solid. (Yield: 86%).

^{1}H-NMR (400 MHz, CD_3CN) δ ppm: 8.34 (d, J=8.2 Hz, 8H, arom), 8.25 (d, J=8.2 Hz, 8H, arom), 8.08 (d, J=8.2 Hz, arom), 7.99 (d, J=8.2 Hz, arom), 7.90 (s, 8H, arom), 7.82 (s, 8H, arom), 4.05 (dd, 8H, CH_2), 3.64-3.57 (m, 8H, CH_2), 3.32 (s, 12H, CH_3), 3.30 (s, 12H, CH_3), 3.24-3.15 (m, 8H, CH_2), 3.09 (dd, 8H, CH_2), 2.36-2.28 (m, 16H, CH_2), 2.09 (s, 6H, AcO), 2.08 (s, 6H, AcO), 1.41 (s, 6H, CH_3), 1.35 (s, 6H, CH_3).

^{13}C-NMR (100 MHz, $CDCl_3$) δ ppm: 177.80 (C=O, AcO), 177.77 (C=O, AcO), 141.49 (arom), 141.30 (arom), 140.14 (arom), 139.90 (arom), 134.18 (arom), 134.12 (arom), 133.67 (arom), 133.62 (arom), 128.45 (arom), 128.32 (arom), 128.19 (arom), 128.06 (arom), 123.64 (CF_3SO_3), 120.46 (CF_3SO_3), 65.81 (-CH_2-), 65.73 (-CH_2-), 61.21 (-CH_2-), 59.32 (-CH_2-), 59.20 (-CH_2-), 51.41 (-CH_3), 51.22 (-CH_3), 43.95(-CH_3), 43.84 (-CH_3), 24.65 (-CH_3, AcO), 24.57 (-CH_3, AcO).

HRMS (*m/z*): calculated 565.1851, found 565.1864 for ($\{Pd_2(Me_2ppp)(AcO)_2\}^{+2}$); calculated 1279.3226, found 1279.3247 for ($\{Pd_2(Me_2ppp)(AcO)_2(CF_3SO_3)_1\}^{+1}$).

1.7. Synthesis and characterization of dinuclear Cu^{II} molecular clip $[Cu_2(Me_2ppp)(OTf)_2](OTf)_2$

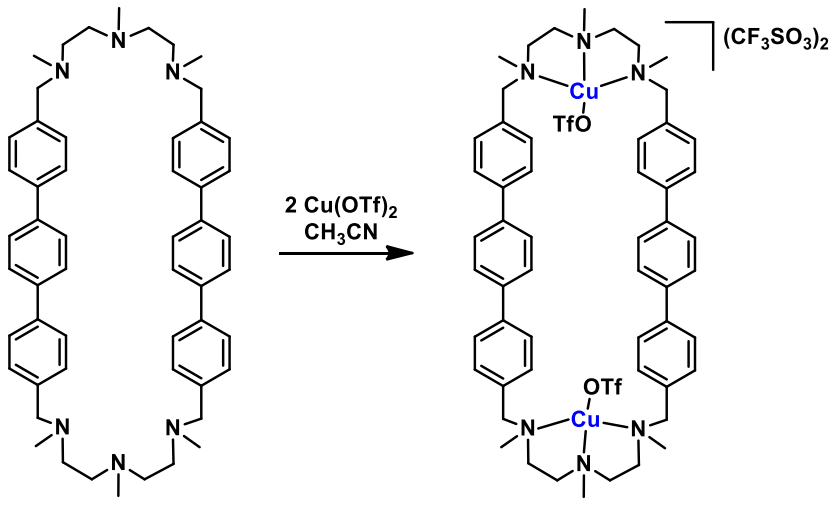

Supplementary Figure 6. Synthesis of $[Cu_2(Me_2ppp)(OTf)_2](OTf)_2$.

In a 20 ml glass vial, 0.095 g of Me_2ppp (1 mmol) and 0.090 g of $Cu(CF_3SO_3)_2$ (2 mmols) were dissolved in 8.5 ml of CH_3CN. The mixture was stirred at room temperature for 16 h. After this time, the reaction crude was filtered through Celite and recrystallized by slow

diffusion of diethyl ether. The product was obtained as a blue crystalline solid. (Yield: 93%).

HRMS (*m/z*): calculated 612.1478, found 612.1465 for ($\{Cu_2(Me_2ppp)(CF_3SO_3)_2\}^{+2}$); calculated 1373.2481, found 1373.2401 for ($\{Cu_2(Me_2ppp)(CF_3SO_3)_3\}^{+1}$).

1.8. Synthesis and characterization of Pd^{II}-based tetragonal prismatic nanocapsule 8·$(BArF)_8$

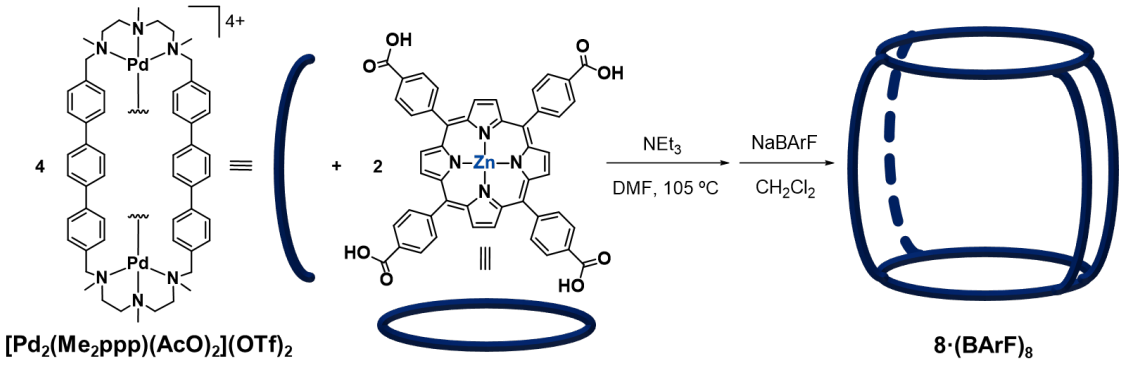

Supplementary Figure 7. Schematic representation for the synthesis of **8**·$(BArF)_8$ nanocapsule.

0.09 g of 5,10,15,20-tetrakis(4-carboxyphenyl)porphyrin-Zn^{II} (2 mmols) were added in a 50 ml round-bottom flask and dissolved in 8 ml of DMF. Then, 76 µl of triethylamine dissolved in 4 ml of DMF were added to the porphyrin solution. Finally, 0.23 g of molecular clip $[Pd_2(Me_2ppp)(AcO)_2](CF_3SO_3)_2$ (4 mmols) dissolved in 20 ml of DMF were added to the reaction mixture and the solution was heated at 105 °C under reflux for 24 h. The reaction crude was cooled to room temperature, filtered through Celite and recrystallized by diffusion of diethyl ether. The **8**·$(CF_3SO_3)_8$ crystalline solid obtained was suspended in 12 ml of DCM, an excess of NaBArF salt was added (6 to 10 mmols) and the mixture was stirred vigorously for 16 h. The mixture was filtered through Celite and the product was obtained by precipitation by slow diffusion of diethyl ether. (Yield: 72%).

^{1}H-NMR (400 MHz, CD_3CN) δ ppm: 8.71 (s, 16H, pyrrole ring), 8.63 (d, J=8.2 Hz, 8H, arom-porph), 8.41 (d, J=8.2 Hz, 8H, arom-porph), 8.25 (d, J=8.2 Hz, 32H, arom-clip), 8.21 (d, 8H, arom-porph), 8.12 (d, 8H, arom-porph), 8.05 (d, J=8.2 Hz, 32H, arom-clip), 7.76 (s, 32H, arom-clip), 7.68-7.65 (m, 96H, $BArF^-$), 4.07 (d, J=13 Hz, 16H, -CH_2-), 3.69 (m, 16H, -CH_2-), 3.59 (s, 48H, N-CH_3), 3.15 (d, J=13 Hz, 16H, -CH_2-), 2.47 (dd, J=13.5 Hz, 16H, -CH_2-), 2.39 (dd, J=13.5 Hz, 16H, -CH_2-), 1.56 (s, 24H, N-CH_3).

^{13}C-NMR (100 MHz, $CDCl_3$) δ ppm: 161.86 (BArF), 149.62 (pyrrole ring), 134.67 (BArF), 134.04 (arom-porph), 132.97 (arom-clip), 131.50 (pyrrole ring), 127.37 (arom-porph),

127.37 (arom-clip), 125.81 (arom-porph), 123.11 (arom-clip), 117.32 (BArF), 64.50 (-CH_2-), 59.99 (-CH_2-), 58.36 (-CH_2-), 51.47 (-CH_3), 43.05 (-CH_3).

HRMS (*m/z*): calculated 718.4442, found 718.4405 for ([**8**·$(BArF)_0$]$^{+8}$); calculated 944.3744, found 944.3704 for ([**8**·$(BArF)_1$]$^{+7}$); calculated 1245.6147, found 1245.6103 for ([**8**·$(BArF)_2$]$^{+6}$); calculated 1667.5511, found 1667.5432 for ([**8**·$(BArF)_3$]$^{+5}$); calculated 2300.2057, found 2300.1789 for ([**8**·$(BArF)_4$]$^{+4}$).

1.9. Synthesis and characterization of Cu^{II}-based tetragonal prismatic nanocapsule 9·$(BArF)_8$

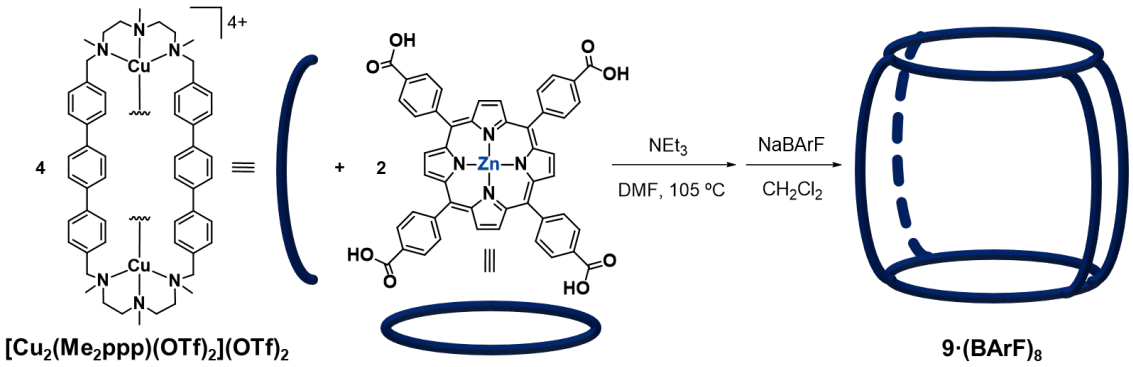

Supplementary Figure 8. Schematic representation for the synthesis of **9**·$(BArF)_8$ nanocapsule.

9.2 mg of 5,10,15,20-tetrakis(4-carboxyphenyl)porphyrin-Zn^{II} (2 mmols) were weighted in a 20 ml glass vial and dissolved in 1.0 ml of DMF. Then, 7.5 µl of triethylamine dissolved in 0.5 ml of DMF were added to the porphyrin solution. Finally, 24.6 mg of molecular clip $[Cu_2(Me_2ppp)(CF_3SO_3)_2](CF_3SO_3)_2$ (4 mmols) dissolved in 2.5 ml of DMF were added to the mixture and the solution was stirred at room temperature for 16 h. The reaction crude was filtered through Celite and recrystallized by diethyl ether diffusion. Product **9**·$(CF_3SO_3)_8$ was obtained as a crystalline solid and suspended in 12 ml of DCM. An excess of NaBArF salt was added (6 to 10 mmols) and the mixture was stirred vigorously for 16 h. The mixture was filtered through Celite and the product was obtained by precipitation with slow diffusion of diethyl ether. (Yield: 75%).

HRMS (*m/z*): calculated 675.5940, found 675.5879 for ([**9**·$(BArF)_0$]$^{+8}$); calculated 895.4028, found 895.3954 for ([**9**·$(BArF)_1$]$^{+7}$); calculated 1188.4811, found 1188.4734 for ([**9**·$(BArF)_2$]$^{+6}$); calculated 1598.7908, found 1598.7825 for ([**9**·$(BArF)_3$]$^{+5}$); calculated 2214.5054, found 2214.4970 for ([**9**·$(BArF)_4$]$^{+4}$).

1.10. Extract encapsulation procedure

Encapsulation in solution. 15 mg of **X**·$(BArF)_8$ (X = 4,6,7,8,9) (1 mmol) were weighted and dissolved in 222 µl of acetonitrile. Then 100 mmols of fullerene extract, containing 60% C_{60}, 28% C_{70} and 2% higher fullerenes, in 2000 µl toluene were added. The mixture was stirred at room temperature for 7 days and analysed by HR-ESI-MS.

Solid state encapsulation. 15 mg of **X**·$(BArF)_8$ (X = 4,6,7,8,9) (1 mmol) were weighted. Then 100 mmols of fullerene extract in toluene, containing 60% C_{60}, 28% C_{70} and 2% higher fullerenes, were added. The mixture was stirred at room temperature for 12 hours and analysed by HR-ESI-MS, and then for 7 days and analysed again by HR-ESI-MS.

a. Fullerene extract + 7·(BArF)$_8$

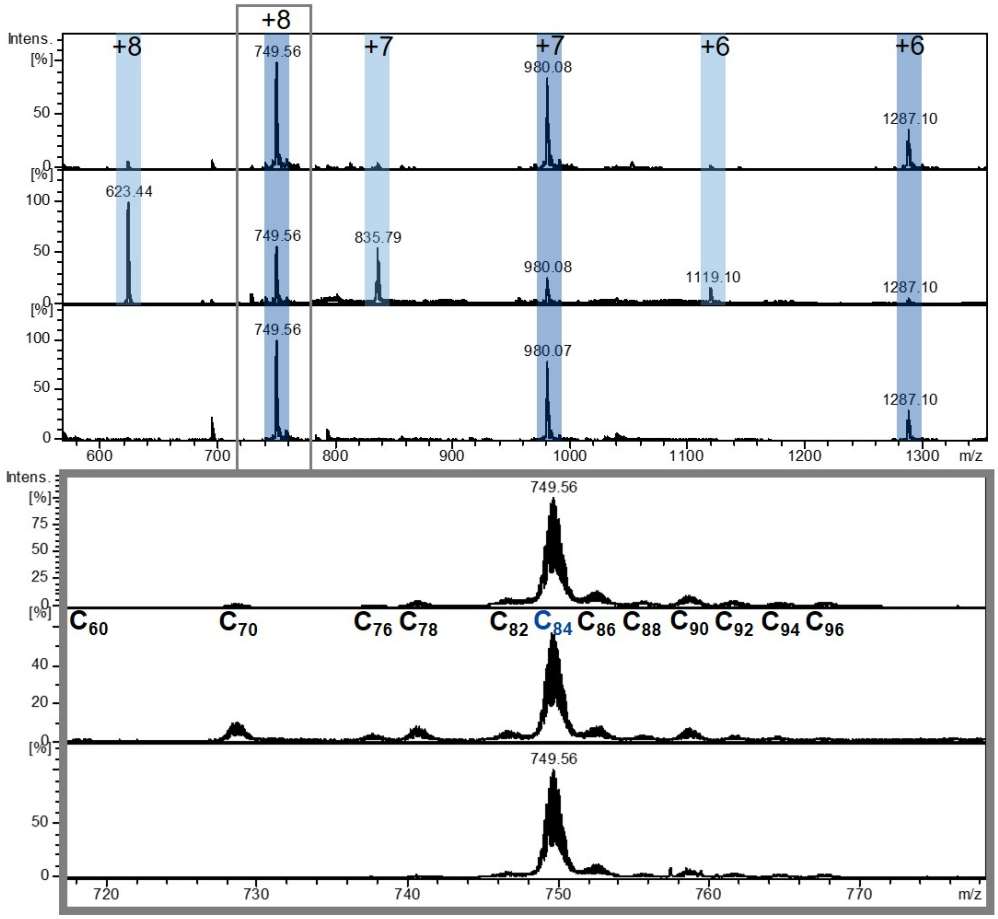

Supplementary Figure 9. HR-MS-ESI. a) **7**·(BArF)$_8$ in solution (toluene:CH_3CN 9:1), 100 eq. of fullerene extract, r.t., 7 days. b) **7**·(BArF)$_8$ in the solid state (suspension in toluene), 100 eq. of fullerene extract, r.t., 12 hours. c) **7**·(BArF)$_8$ in the solid state (suspension in toluene), 100 eq. of fullerene extract, r.t., 7 days.

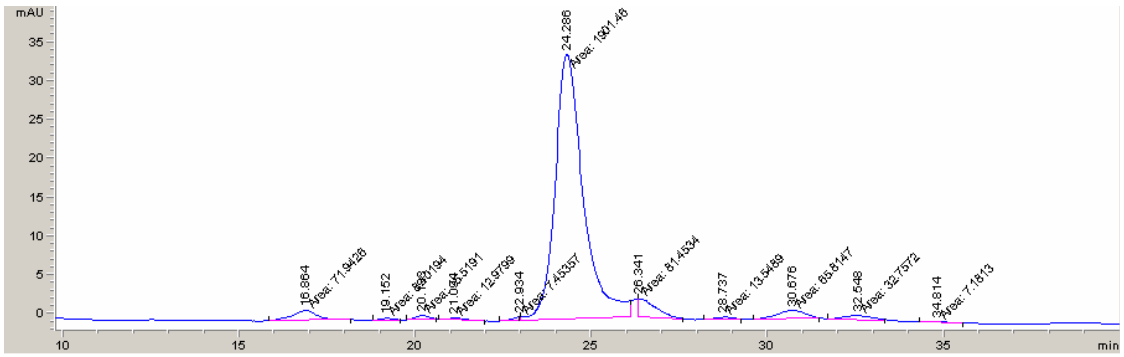

Supplementary Figure 10. HPLC after the addition of 20 eq. of TfOH to **7**·(BArF)$_8$ and solubilizing the C_{84} and other higher fullerenes in toluene.

Supplementary Table 1. HPLC data.

	TIME	AREA	HEIGHT	WIDTH	AREA%	SYMMETRY
1	16.86	71.90	1.30	0.92	3.24	1.07
2	19.15	8.40	0.29	0.49	0.37	0.72
3	20.18	15.50	0.54	0.48	0.70	1.12
4	21.09	13.00	0.30	0.72	0.59	0.56
5	22.93	7.50	0.44	0.28	0.34	0.00
6	**24.29**	**1901.50**	**34.10**	**0.93**	**85.71**	**0.71**
7	26.34	81.50	2.30	0.58	3.67	0.03
8	28.74	13.50	0.36	0.63	0.61	1.03
9	30.68	65.80	1.10	0.99	2.97	1.14
10	32.55	32.80	0.55	0.99	1.48	1.01
11	34.81	7.20	0.14	0.89	0.32	0.71

b. Fullerene extract + 6·$(BArF)_8$

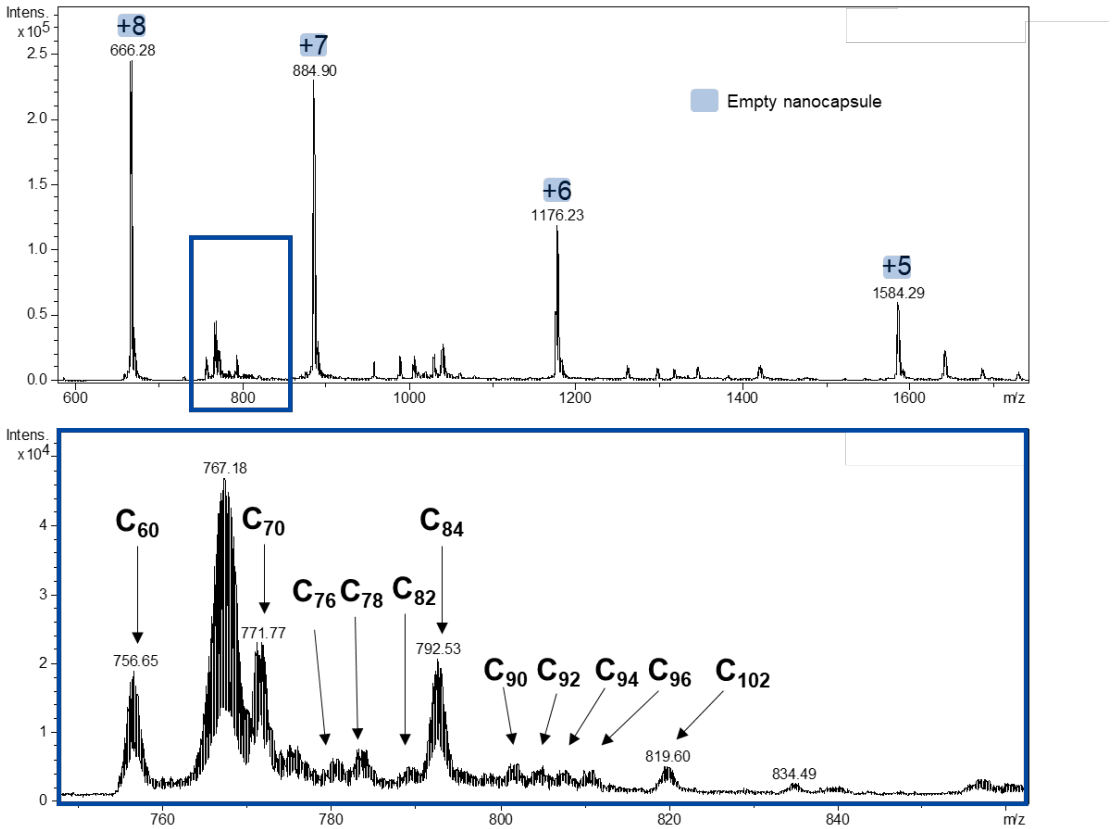

Supplementary Figure 11. HR-MS-ESI after the addition of 100 eq. of fullerene extract to **6**·$(BArF)_8$ at r.t. for 7 days in the solid state (suspension in toluene).

c. Fullerene extract + 8·(BArF)$_8$

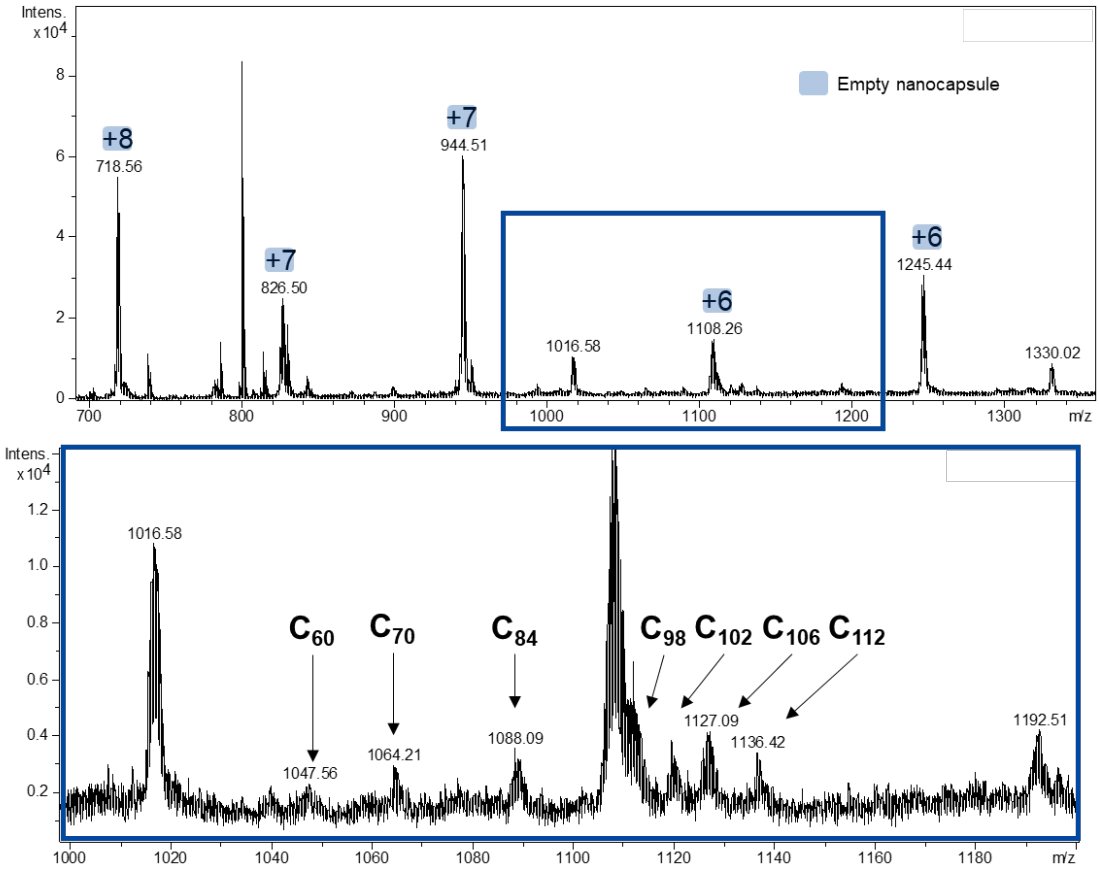

Supplementary Figure 12. HR-MS-ESI after the addition of 100 eq. of fullerene extract to **8**·(BArF)$_8$ at r.t. for 7 days in the solid state (suspension in toluene).

1.11. C_{84} isolation and characterization

a. HPLC-DAD

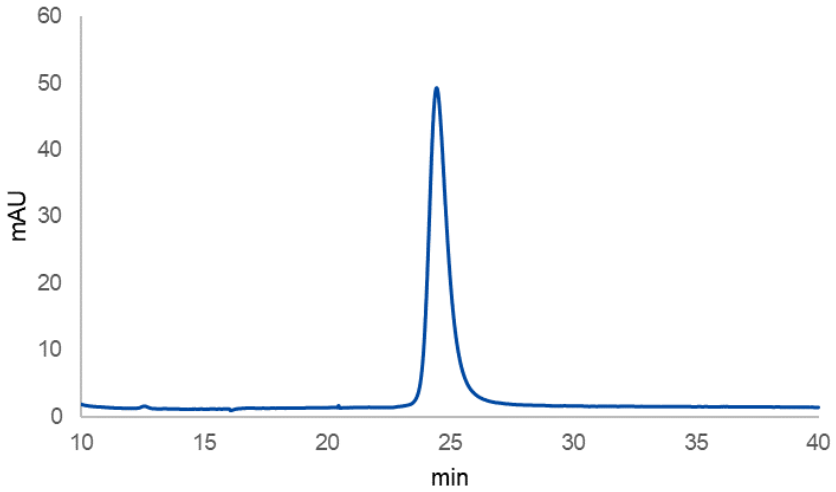

Supplementary Figure 13. HPLC-DAD chromatogram of C_{84} released from nanocapsule **7**·$(BArF)_8$ and collected.

b. UV-Vis

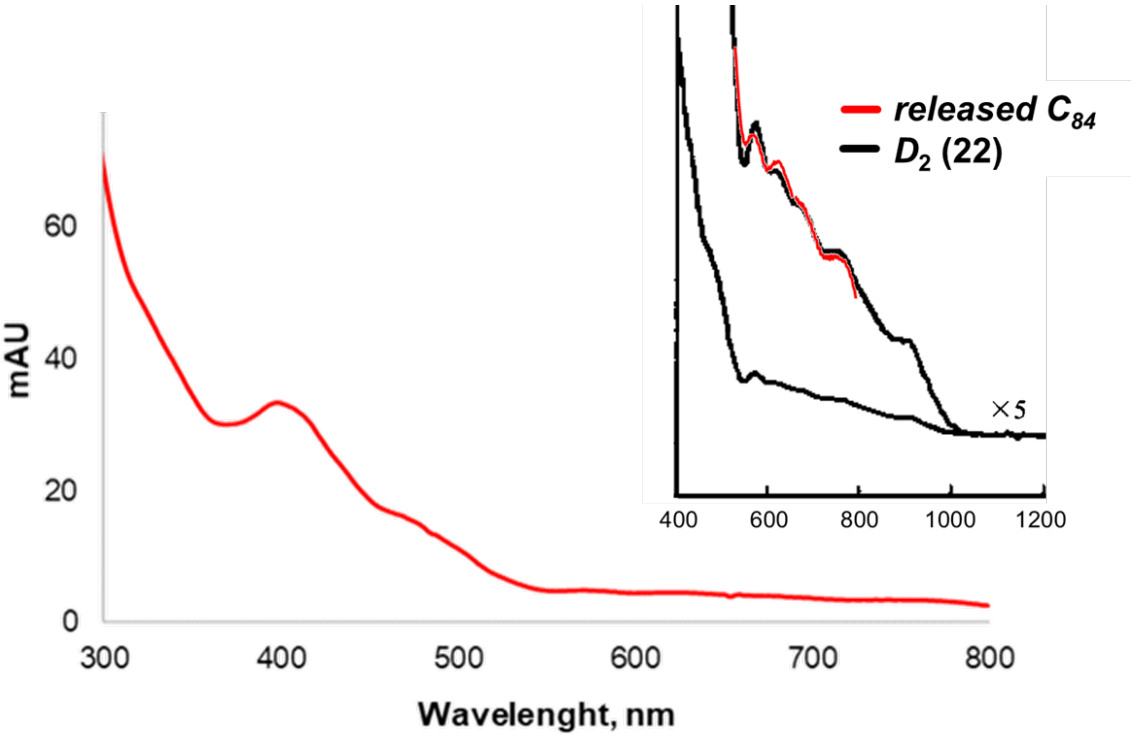

Supplementary Figure 14. (a) UV-Vis spectrum of purified C_{84} and comparison with the reported D_2(22) UV-Vis spectra.

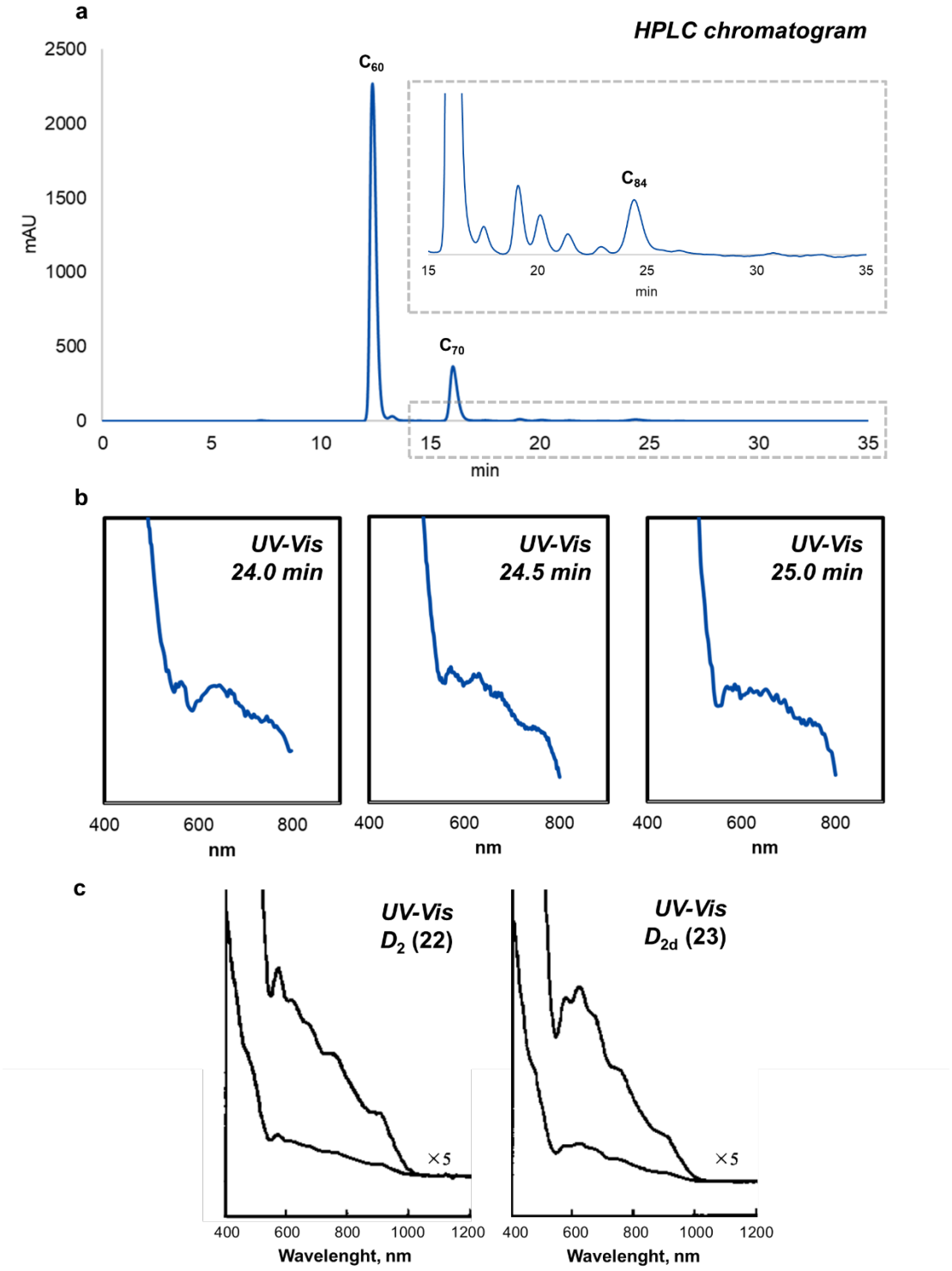

Supplementary Figure 15. (a) HPLC chromatogram of the fullerene extract. (b) UV-Vis spectrum at the head (24.0 min), middle (24.5 min) and tail (25.0 min) of C_{84} peak. (c) UV-Vis spectrum of the reported D_2 (22) and D_{2d} (23) isomers.

c. MALDI-TOF

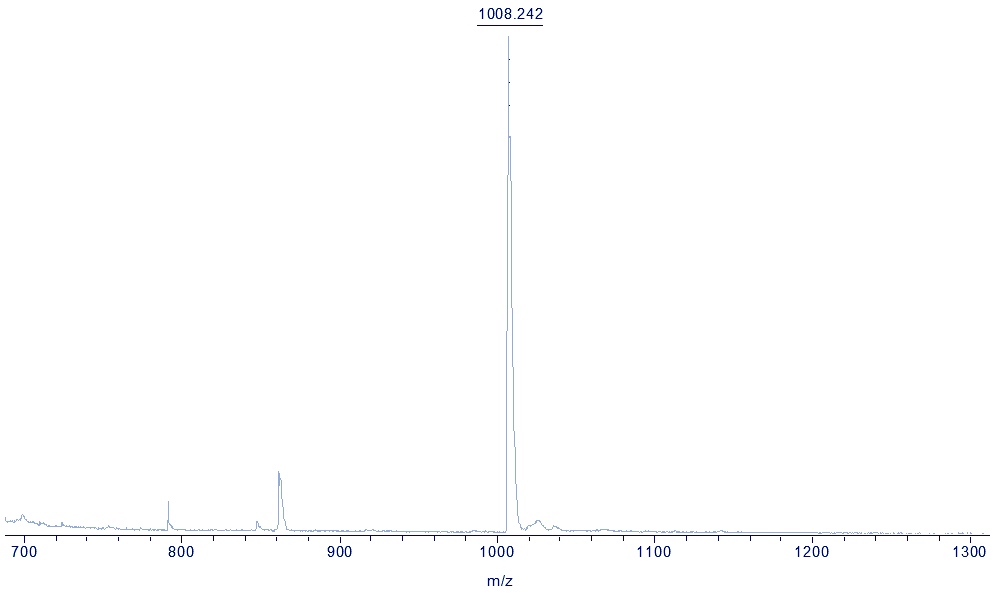

Supplementary Figure 16. MALDI-TOF spectrum of purified C_{84}.

d. ^{13}C-NMR

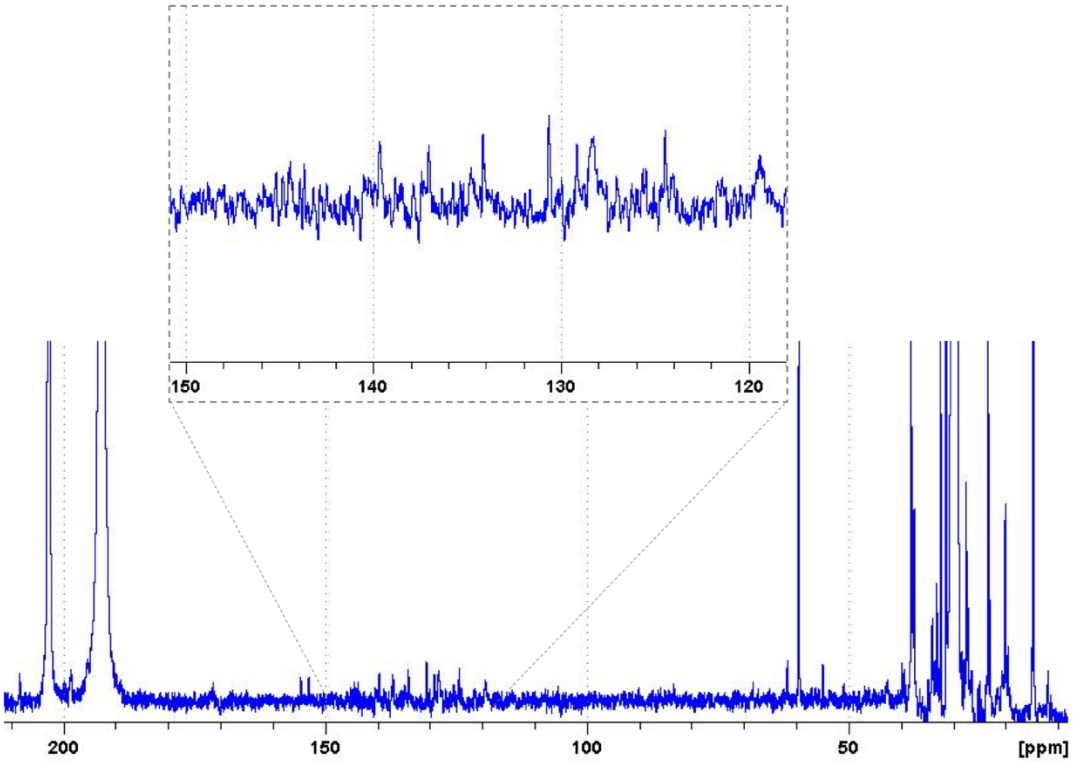

Supplementary Figure 17. ^{13}C-NMR spectrum of the purified C_{84} registered with a 500 MHz NMR (equipped with a cryoprobe) for 3 days (1.6·x 105 scans, CS_2:acetone-d6, 40 mM $Cr(acac)_3$ as relaxing agent, d1 = 2s).

e. $C_{84}\subset 7\cdot(BArF)_8$

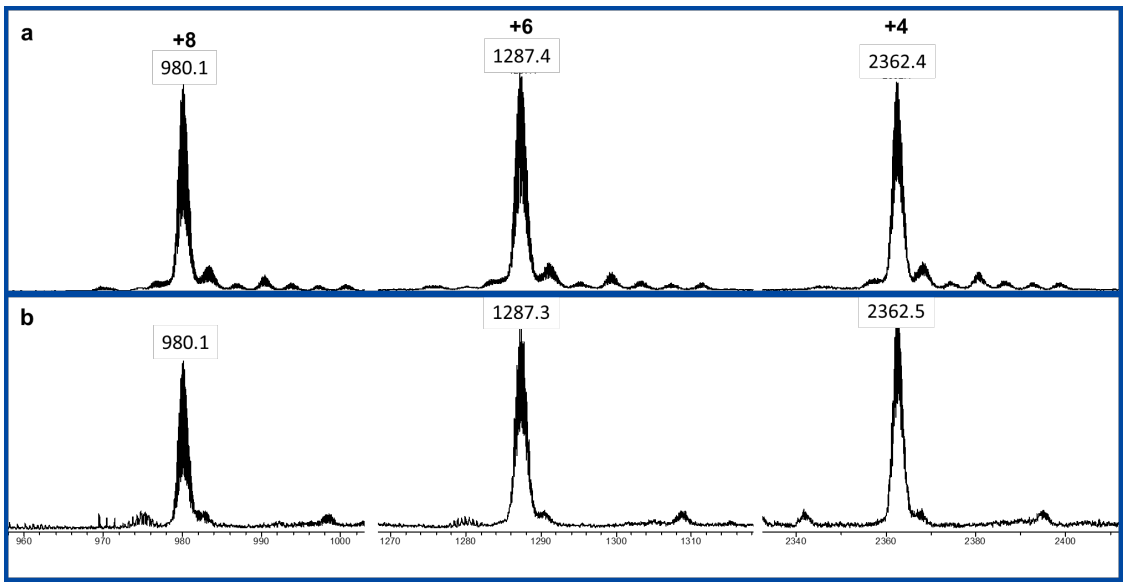

Supplementary Figure 18. HR-MS-ESI after encapsulation of fullerene extract (a) and after encapsulation of the purified C_{84} to **7**·$(BArF)_8$ (b).

1.12. C_{84} binding constant calculation

a. $C_{84}\subset$ 7·$(BArF)_8$ + 8·$(BArF)_8$

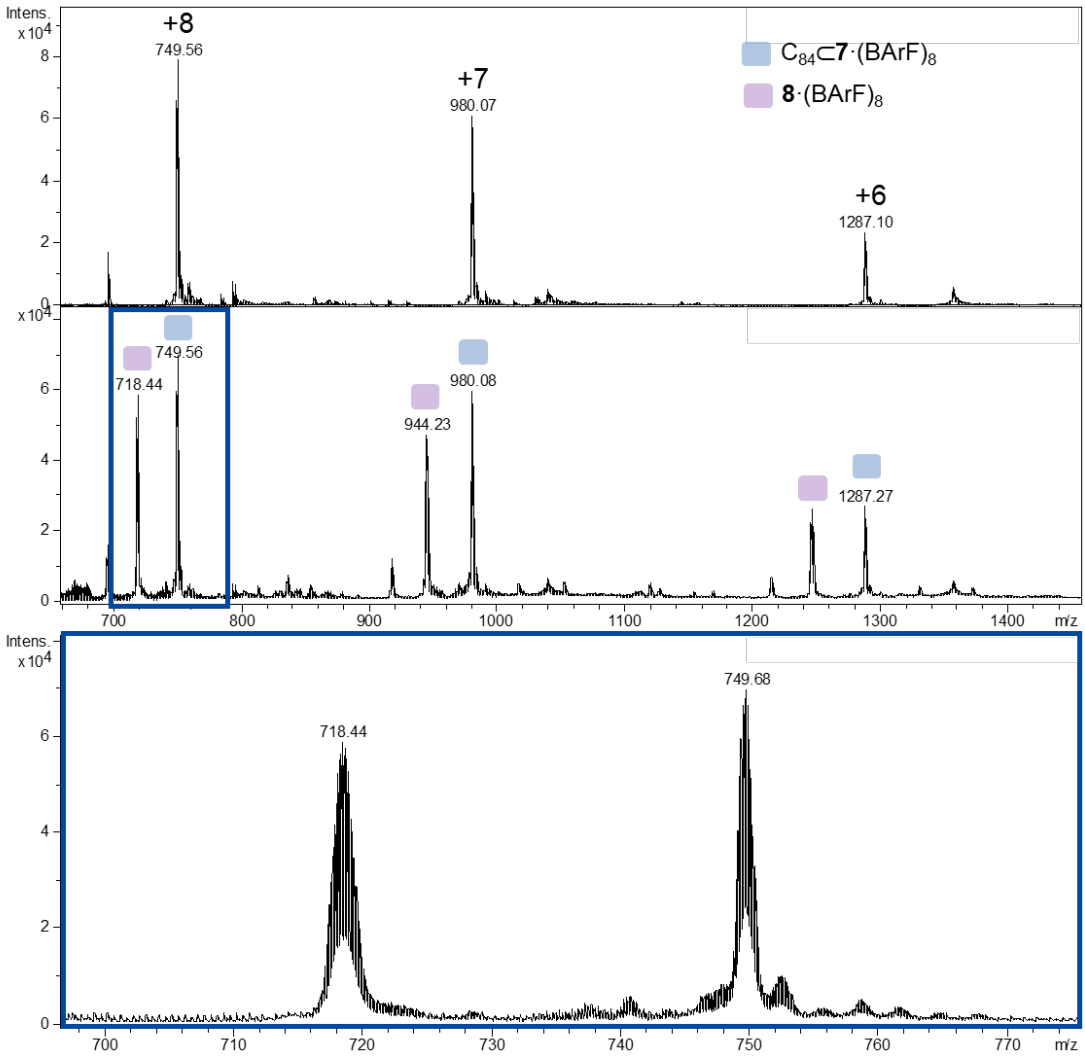

Supplementary Figure 19. HR-MS-ESI of the encapsulation of fullerene extract (C_{84} mainly) with 15 mg of **7**·$(BArF)_8$ (in the solid state) (top), HR-MS-ESI of the addition of **8**·$(BArF)_8$ into the $C_{84}\subset$ **7**·$(BArF)_8$ solution (center) and zoom of the latter (bottom).

b. $(C_{59}N)_2$⊂ 7·$(BArF)_8$ + fullerene extract (100 eq., 4d, toluene)

(1) Encapsulation of $(C_{59}N)_2$ into **6**·$(BArF)_8$. **(2)** Addition of fullerene extract (100 eq) in toluene and stirring at room temperature for 4 days.

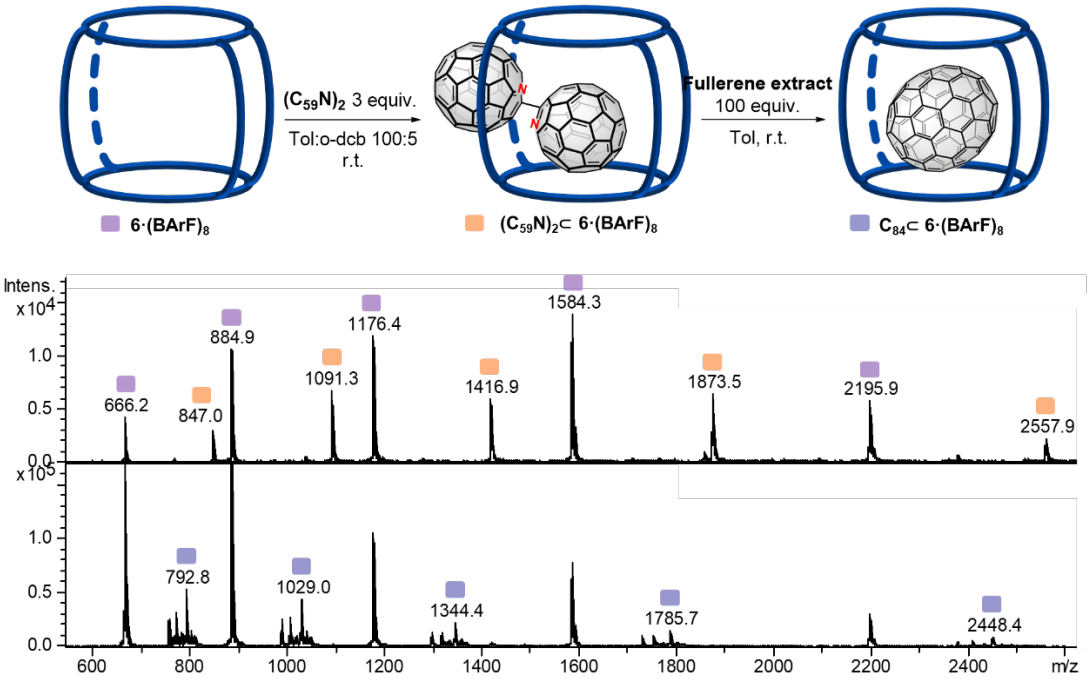

Supplementary Figure 20. HR-MS-ESI of $(C_{59}N)_2$⊂**6**·$(BArF)_8$ (top) and after exchanging with C_{84} (bottom).

1.13. UV-Vis titrations

Experimental procedure and general remarks

All titrations were performed in a mixture of PhMe/MeCN/*o*-DCB (9:1:0.09, v/v) at room temperature, on an Agilent 8452 UV-vis spectrophotometer using a 1 cm quartz cell. Concentration of either host or guest species was kept constant over the course of titration. Titration data was fitted by using the online calculator Bindfit (http://supramolecular.org).[5]

Supplementary Table 2. Comparison of different binding constants. Solvent: PhMe/MeCN/*o*-DCB (9:1:0.09).

NANOCAPSULE	K_1 (M^{-1})	K_2 (M^{-1})	K ± ERROR (M^{-1})
4 [ref [1]]	-	-	**9.4 (± 0.5) x 10^5**
6	1.2 x 10^7	8.2 x 10^6	**1.0 (± 1.1) x 10^7**
7	1.7 x 10^6	1.4 x 10^6	**1.6 (± 0.1) x 10^6**
8	5.0 x 10^7	3.6 x 10^7	**4.3 (± 1.0) x 10^7**
9	1.6 x 10^7	9.2 x 10^6	**1.3 (± 0.6) x 10^7**

a. UV-Vis titration: $(C_{59}N)_2$ + 6·$(BArF)_8$

A

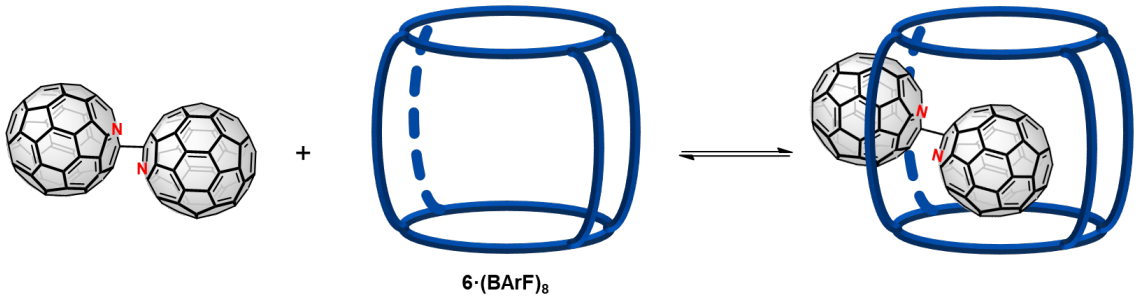

B

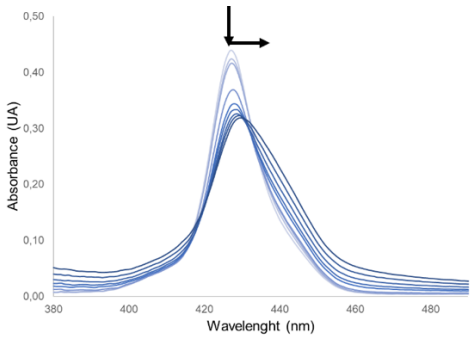

C

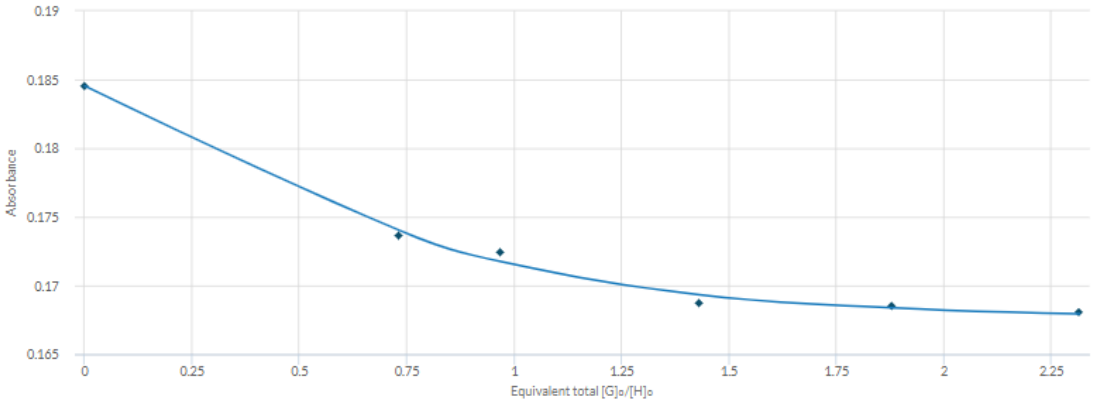

Supplementary Figure 22. Representative titration data for **6**/$(C_{59}N)_2$ host-guest system. Solvent: PhMe/MeCN/*o*-DCB (9:1:0.09). (A) Changes in absorption spectra of **6** (8.3×10^{-7} M, λ_{exc} = 420 nm) upon addition of diazafullerene $(C_{59}N)_2$ (0 – 3.4×10^{-5} M). (B) Fit of the titration data according to 1:1 binding model. See supplementary excel input files "6_T1" and "6_T2" for the detailed report from supramolecular.org page.

b. UV-Vis titration: $(C_{59}N)_2$ + 7·$(BArF)_8$

A

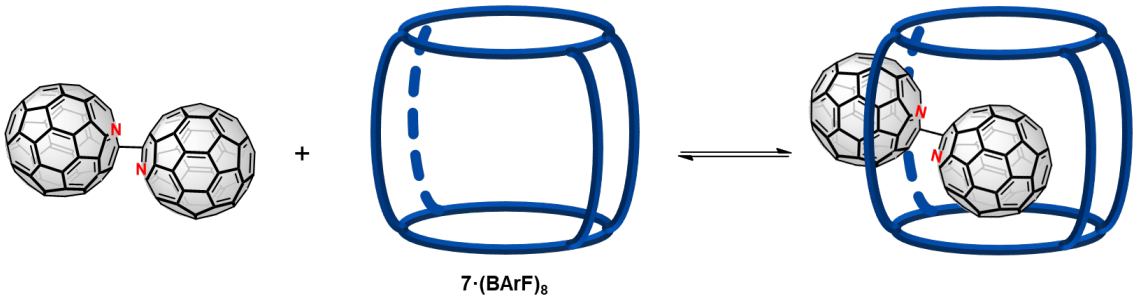

B

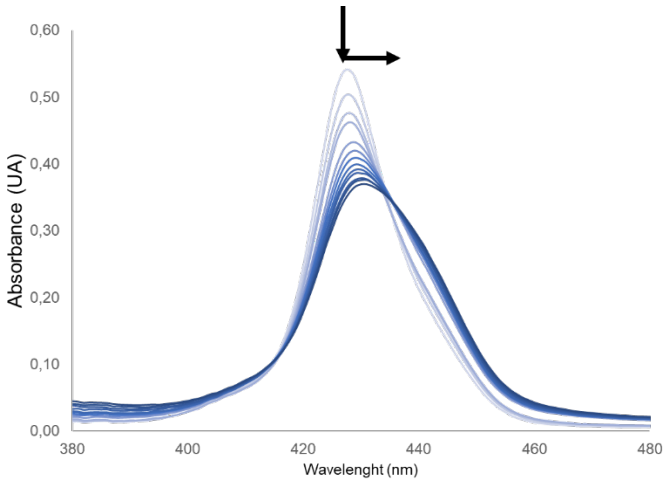

C

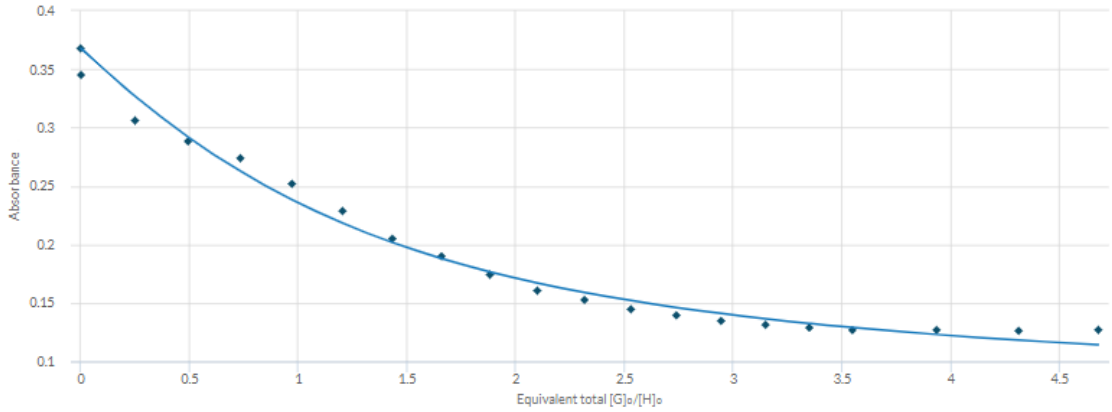

Supplementary Figure 23. Representative titration data for **7**/$(C_{59}N)_2$ host-guest system. Solvent: PhMe/MeCN/*o*-DCB (9:1:0.09). (A) Changes in absorption spectra of **7** (8.3×10^{-7} M, λ_{exc} = 420 nm) upon addition of diazafullerene $(C_{59}N)_2$ (0 – 6.4×10^{-5} M). (B) Fit of the titration data according to 1:1 binding model. See supplementary excel input files "7_T1" and "7_T2" for the detailed report from supramolecular.org page.

c. UV-Vis titration: $(C_{59}N)_2$ + 8·$(BArF)_8$

A

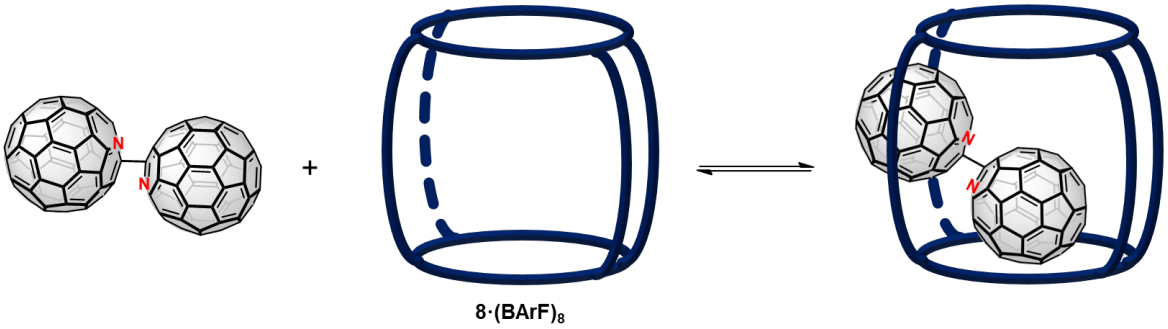

B

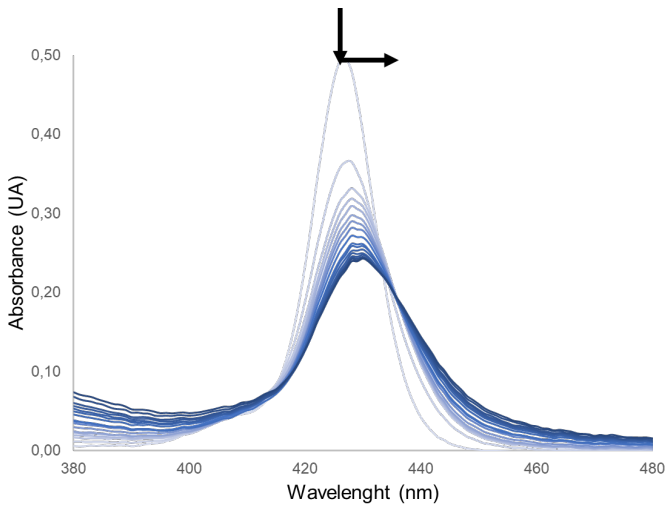

C

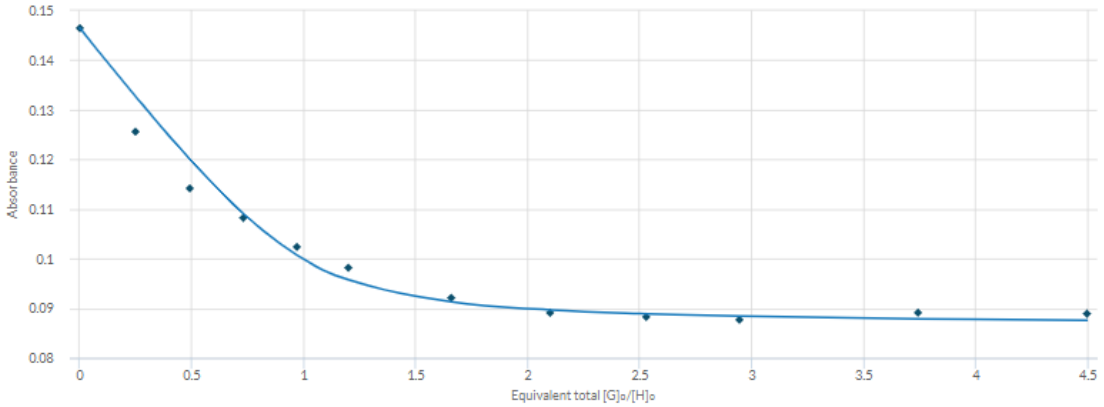

Supplementary Figure 24. Representative titration data for **8**/$(C_{59}N)_2$ host-guest system. Solvent: PhMe/MeCN/*o*-DCB (9:1:0.09). (A) Changes in absorption spectra of **8** (4.3×10^{-7} M, λ_{exc} = 420 nm) upon addition of diazafullerene $(C_{59}N)_2$ (0 – 3.7×10^{-5} M). (B) Fit of the titration data according to 1:1 binding model. See supplementary excel input files "8_T1" and "8_T2" for the detailed report from supramolecular.org page.

d. UV-Vis titration: $(C_{59}N)_2$ + 9·$(BArF)_8$

A

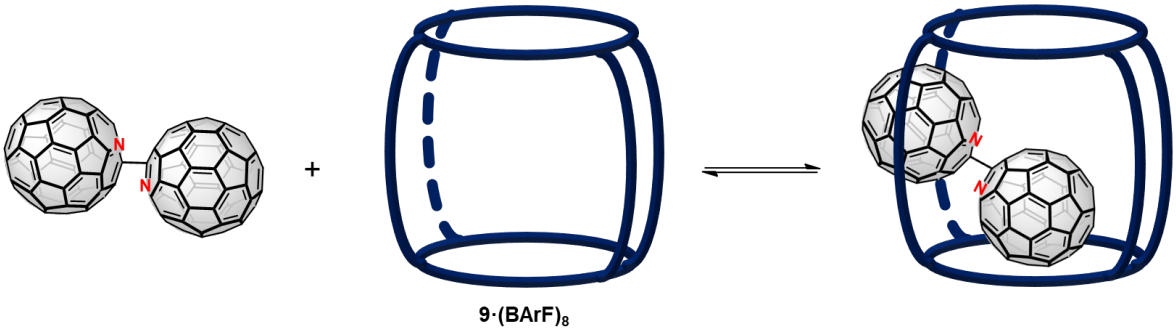

9·$(BArF)_8$

B

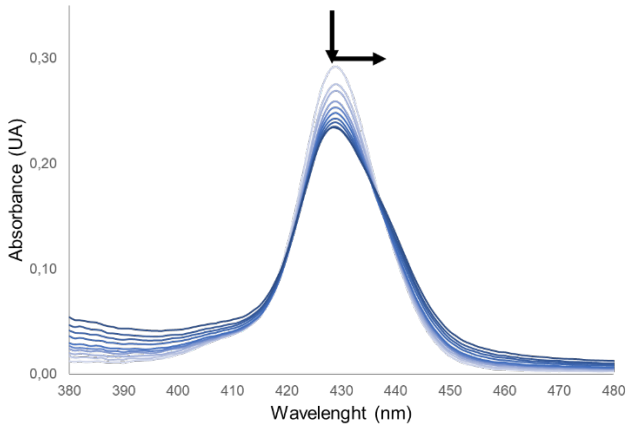

C

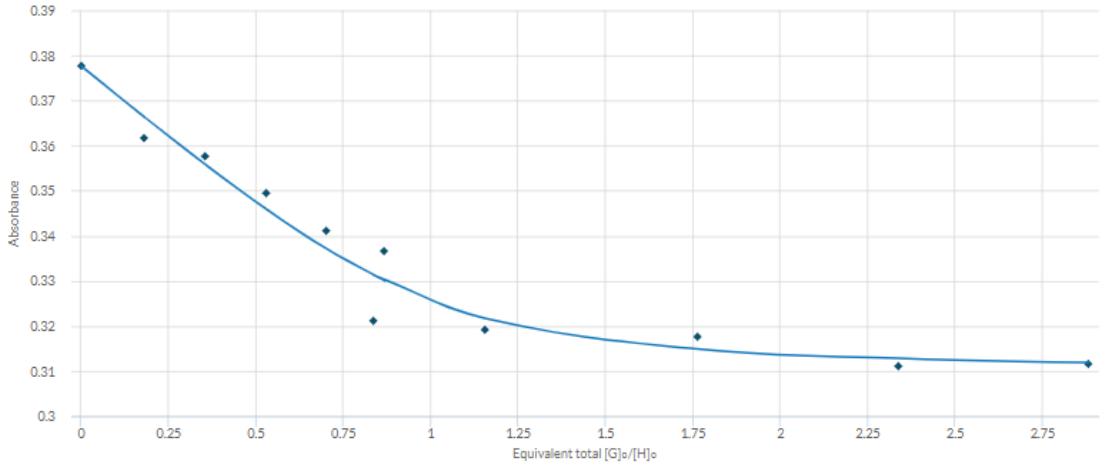

Supplementary Figure 25. Representative titration data for **9**/$(C_{59}N)_2$ host-guest system. Solvent: PhMe/MeCN/*o*-DCB (9:1:0.09). (A) Changes in absorption spectra of **9** (8.3×10^{-7} M, λ_{exc} = 420 nm) upon addition of diazafullerene $(C_{59}N)_2$ (0 – 9.2×10^{-5} M). (B) Fit of the titration data according to 1:1 binding model. See supplementary excel input files “9_T1” and “9_T2” for the detailed report from supramolecular.org page.

2. Supplementary Figures

2.1. Characterization of dialdehyde (ppp)

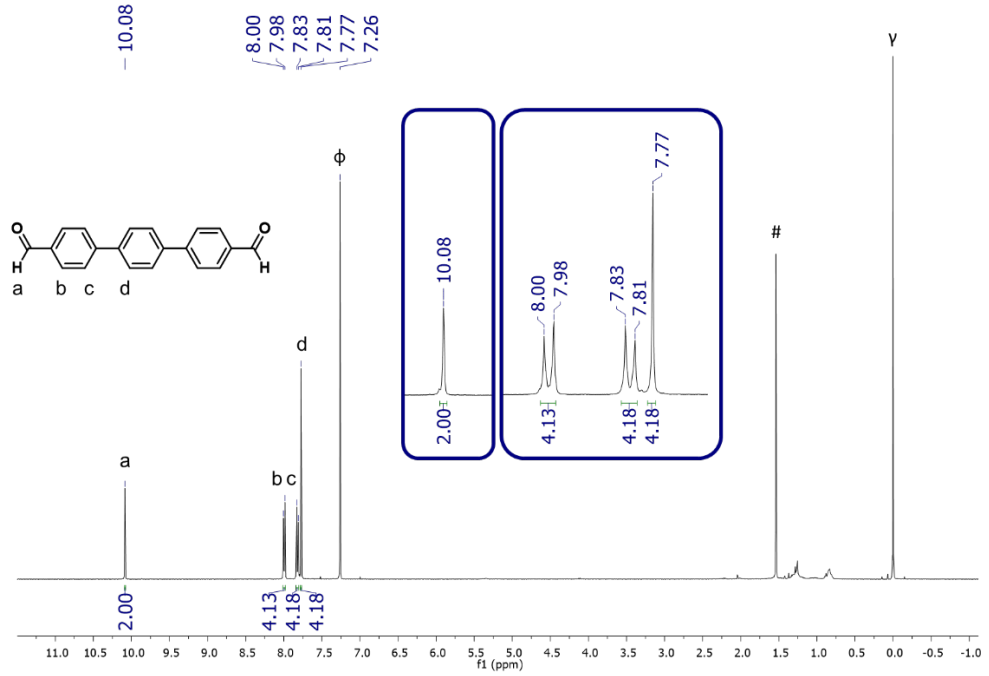

Supplementary Figure 26. ^{1}H-NMR of (1,1':4',1''-terphenyl)-4,4''-dicarbaldehyde (ppp). Experiment performed in $CDCl_3$ at 298 K (400 MHz). (ϕ) $CHCl_3$, (#) H_2O, (γ) TMS.

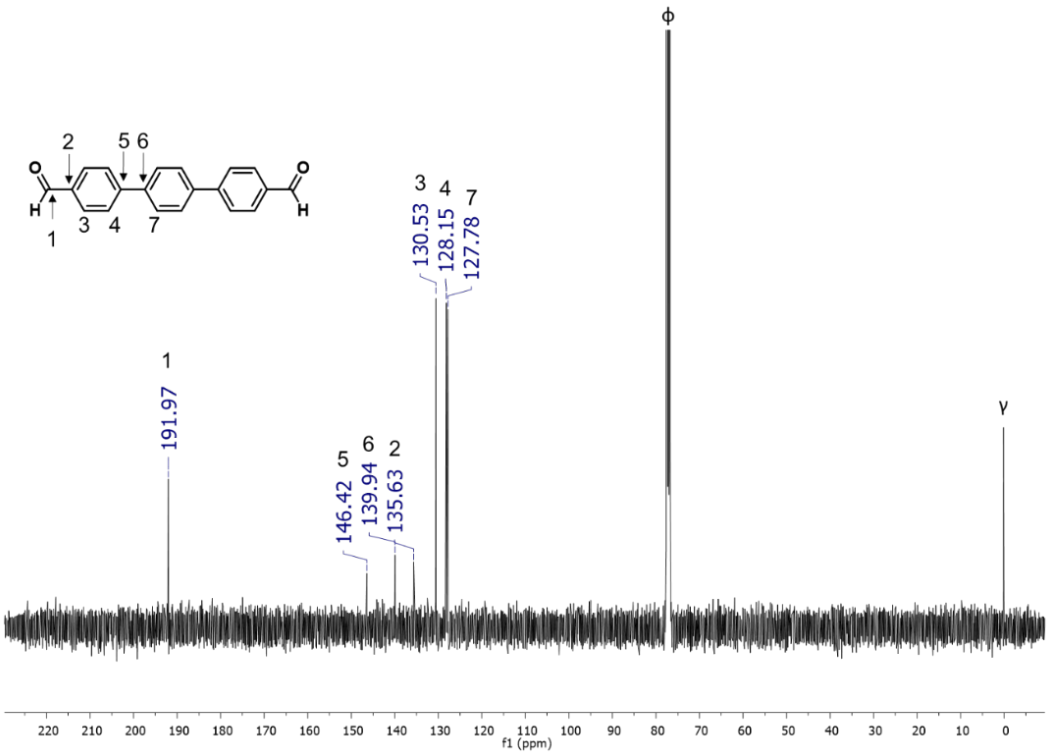

Supplementary Figure 27. ^{13}C-NMR of (1,1':4',1''-terphenyl)-4,4''-dicarbaldehyde (ppp). Experiment performed in $CDCl_3$ at 298 K (100 MHz). (ϕ) $CHCl_3$, (γ) TMS.

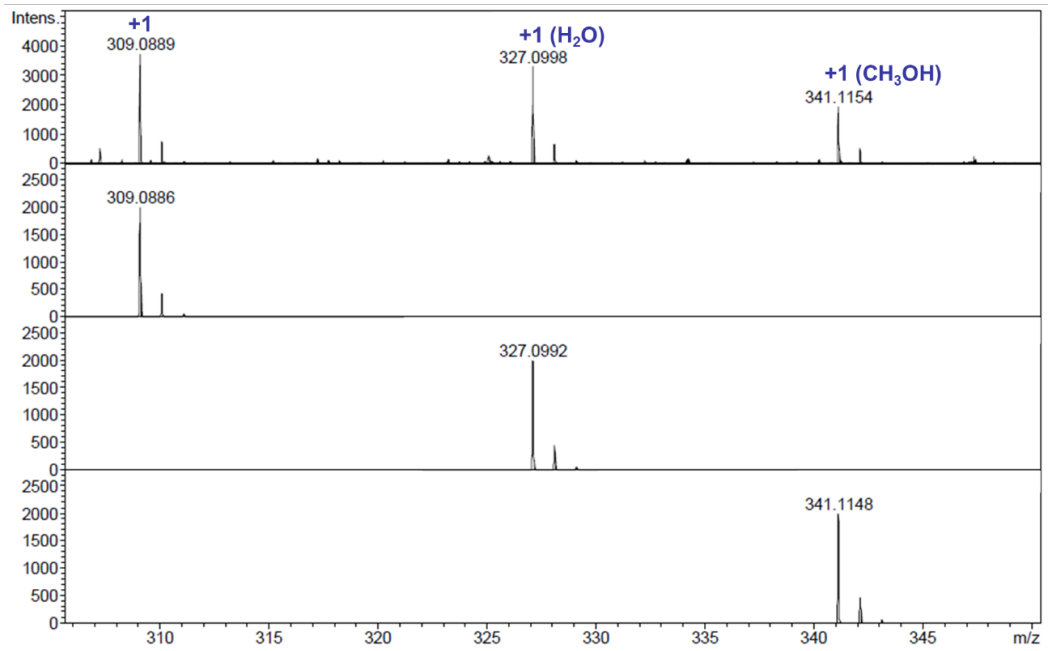

Supplementary Figure 28. HRMS spectrum of (1,1':4',1''-terphenyl)-4,4''-dicarbaldehyde (ppp). Experimental (top) and theoretical isotopic pattern for selected peaks is shown. Sample was dissolved in chloroform and the spectrum was registered on a Bruker Micro TOF-Q-II exact mass spectrometer.

2.2. Characterization of S_2ppp

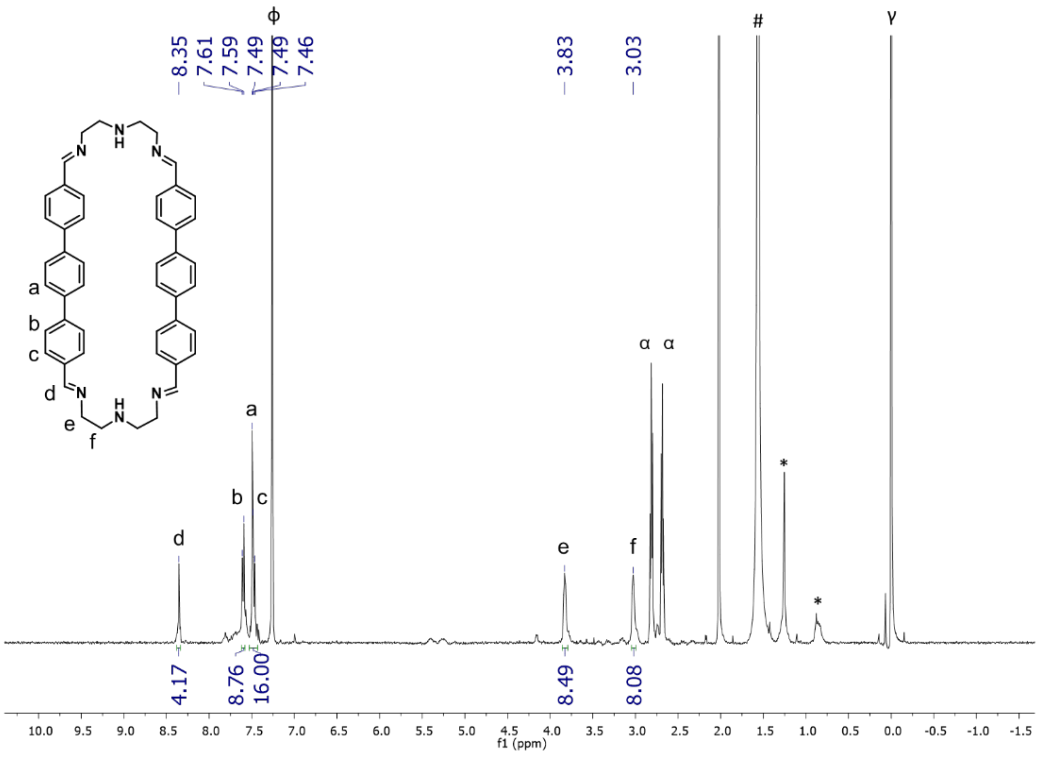

Supplementary Figure 29. ^{1}H-NMR of S_2ppp macrocycle. Experiment was performed in $CDCl_3$ at 298 K (400 MHz). (ϕ) $CHCl_3$, (*) H grease, (γ) TMS, (α) diethylentriamine.

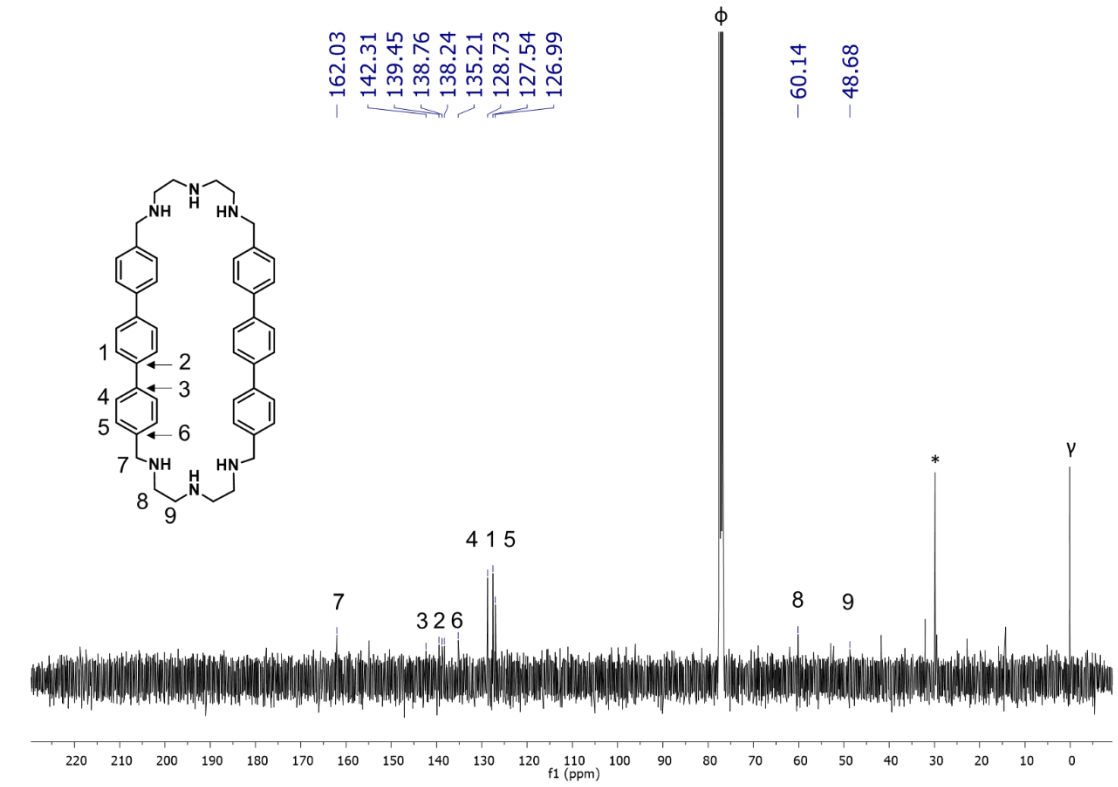

Supplementary Figure 30. ^{13}C-NMR of S_2ppp macrocycle. Experiment was performed in $CDCl_3$ at 298 K (100 MHz). (ϕ) $CHCl_3$, (γ) TMS.

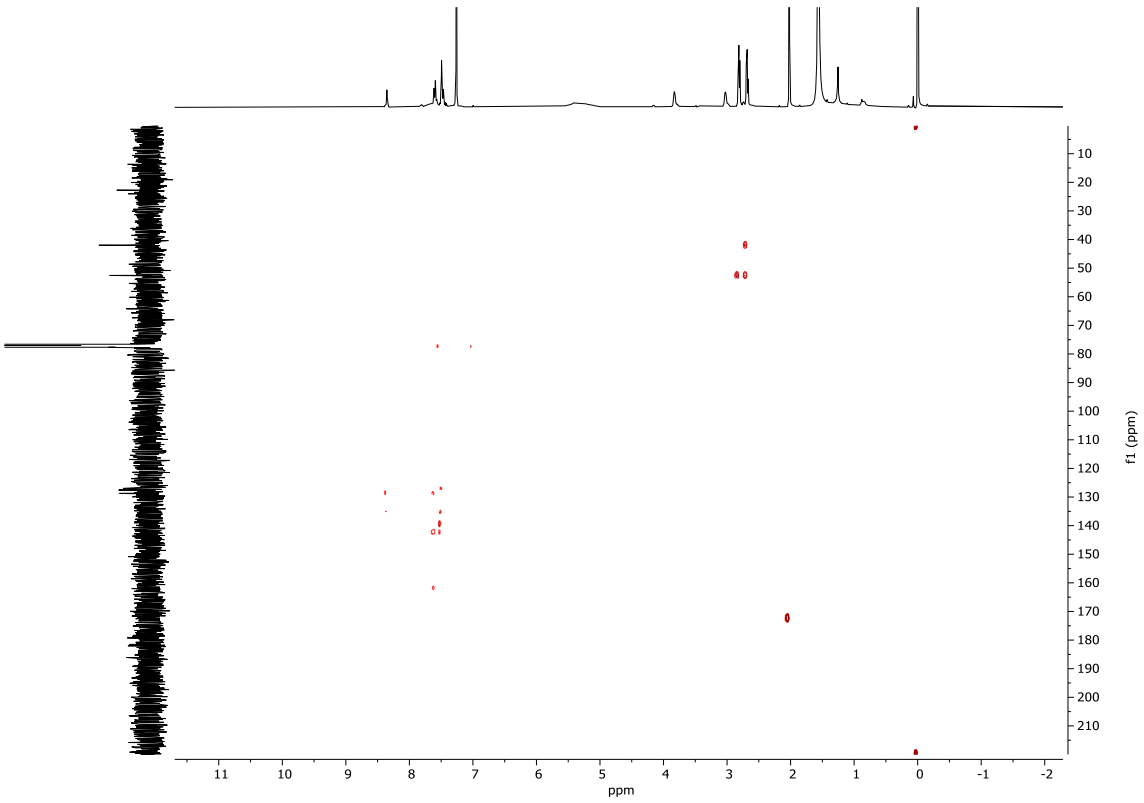

Supplementary Figure 31. HMBC of S_2ppp macrocycle. Experiment was performed in $CDCl_3$ at 298 K (400 MHz).

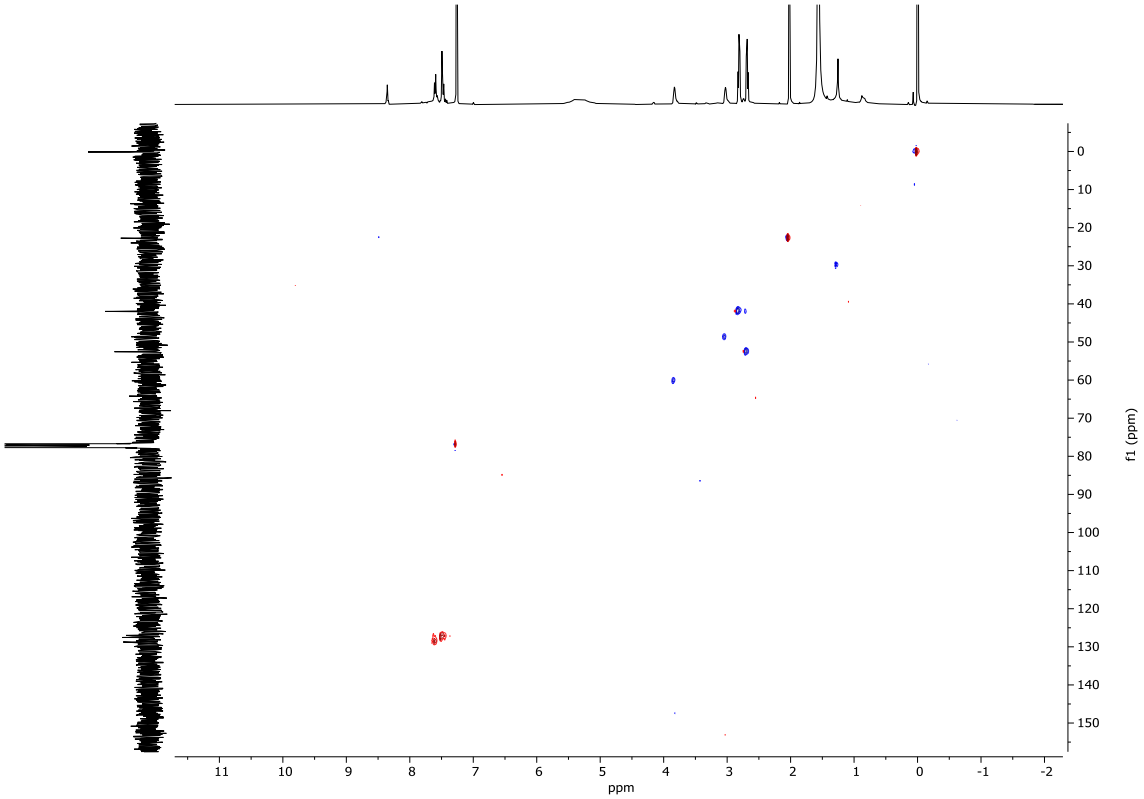

Supplementary Figure 32. HSQC of S_2ppp macrocycle. Experiment was performed in $CDCl_3$ at 298 K (400 MHz).

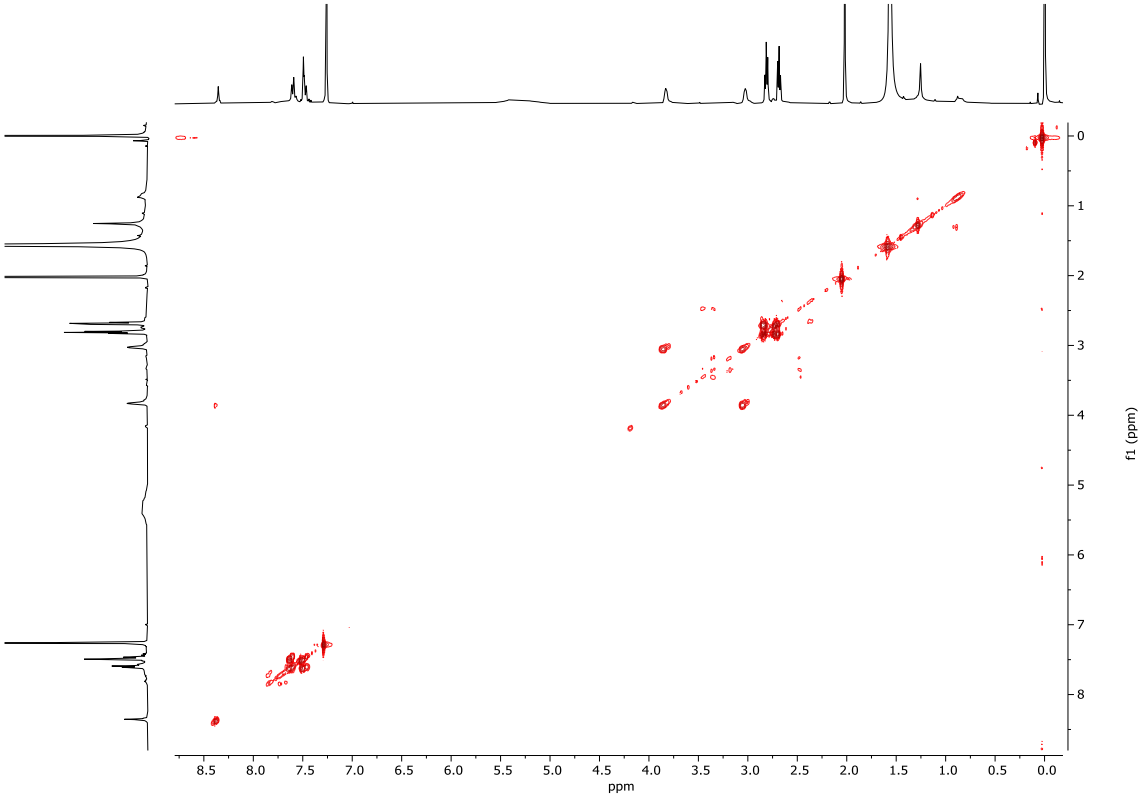

Supplementary Figure 33. COSY of S_2ppp macrocycle. Experiment was performed in $CDCl_3$ at 298 K (400 MHz).

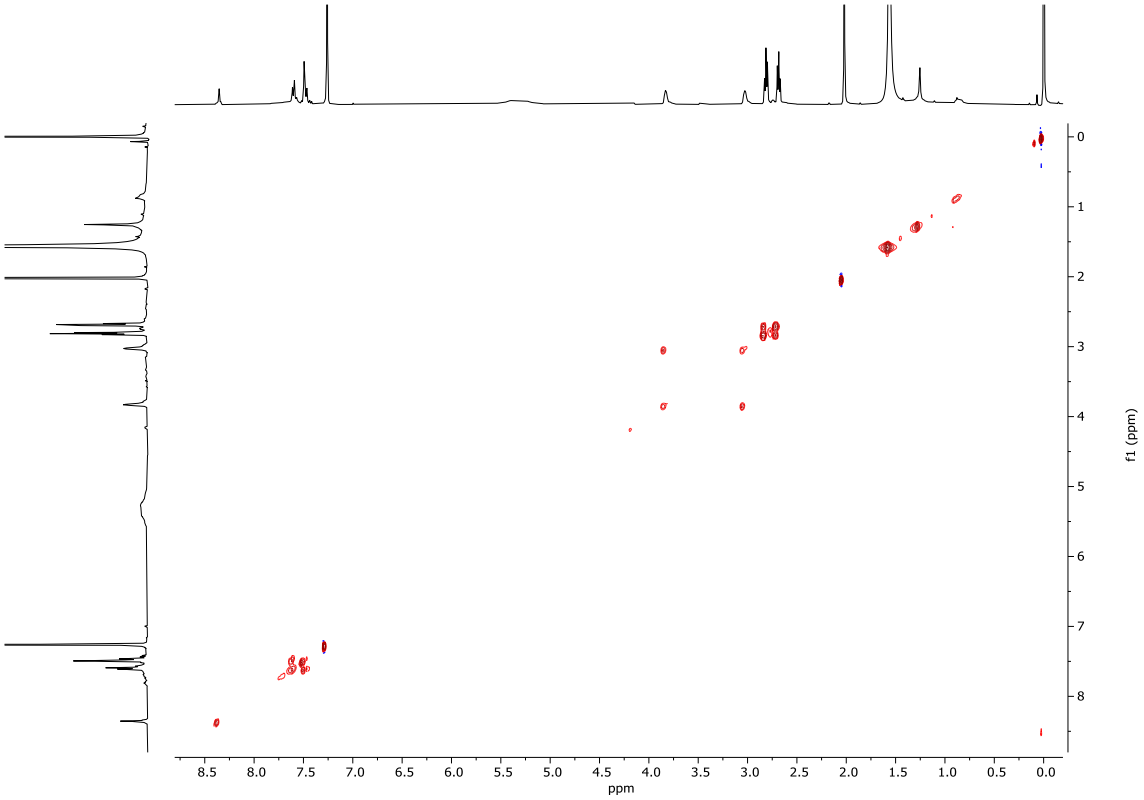

Supplementary Figure 34. TOCSY of S_2ppp macrocycle. Experiment was performed in $CDCl_3$ at 298 K (400 MHz).

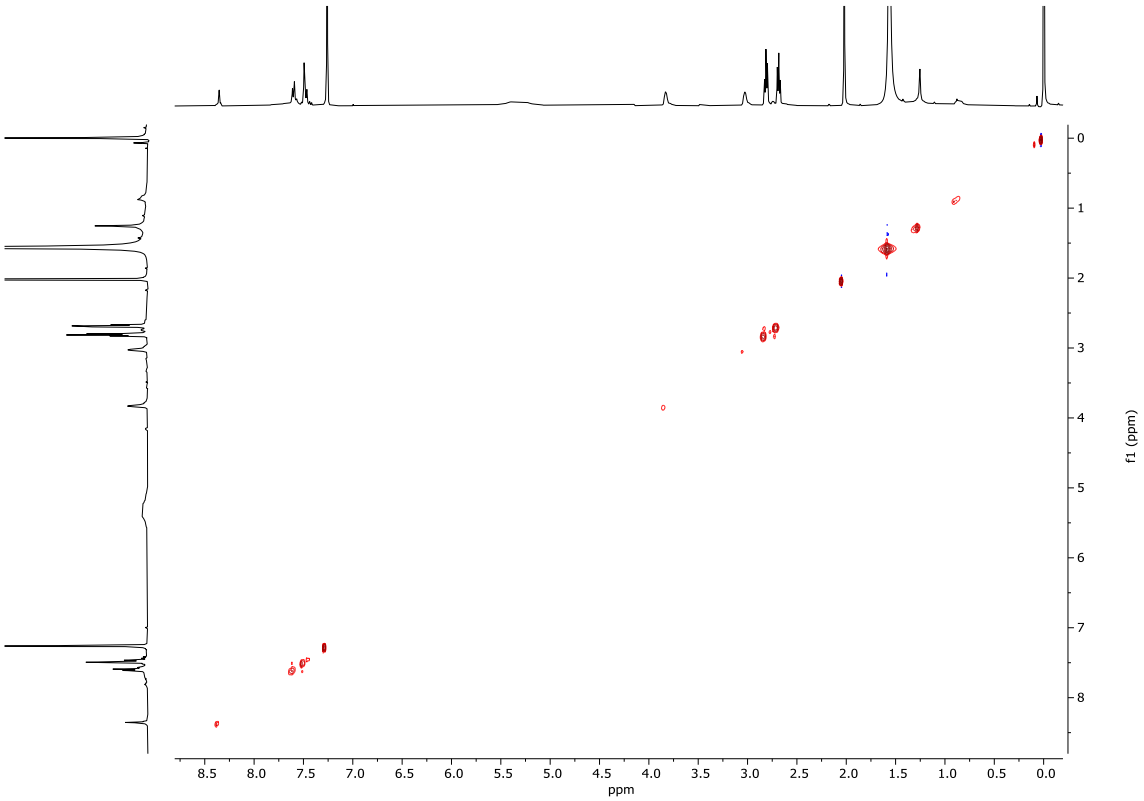

Supplementary Figure 35. NOESY of S_2ppp macrocycle. Experiment was performed in $CDCl_3$ at 298 K (400 MHz).

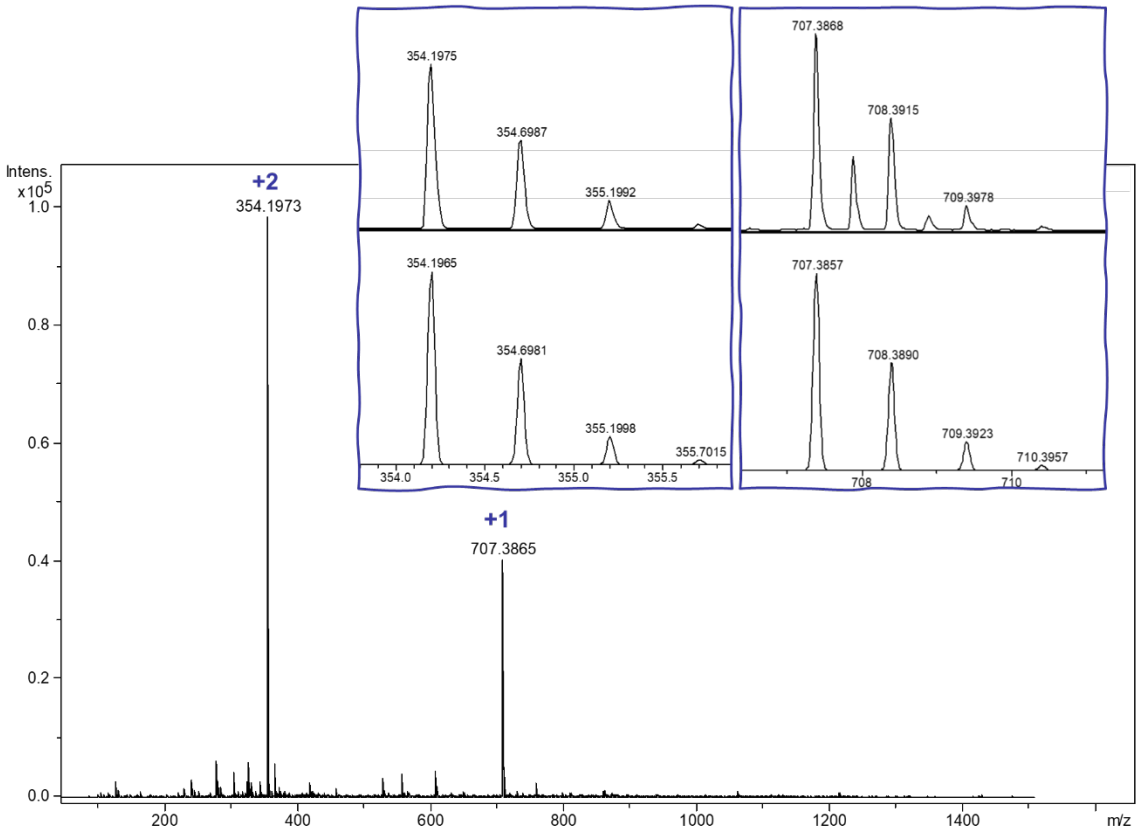

Supplementary Figure 36. HRMS spectrum of S_2ppp macrocycle. Experimental (top) and theoretical (bottom) isotopic pattern for selected peaks is shown. The sample was dissolved in chloroform and the spectrum was registered on a Bruker Micro TOF-Q-II exact mass spectrometer.

2.3. Characterization of H_2ppp

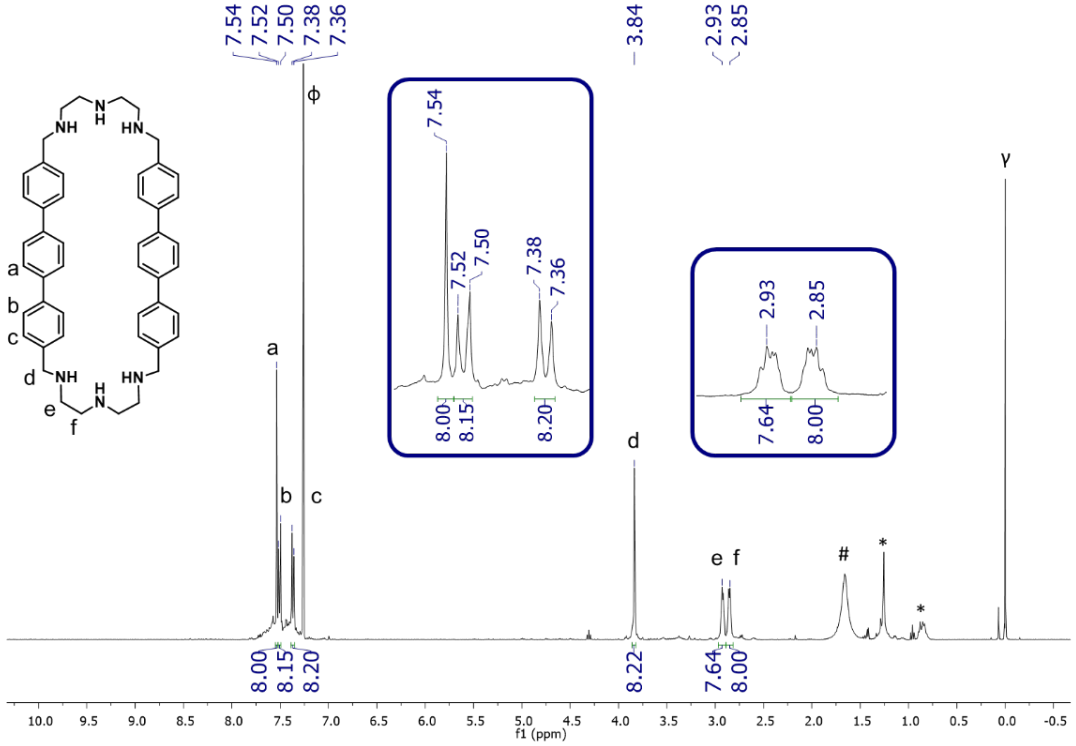

Supplementary Figure 37. ^{1}H-NMR of H_2ppp macrocycle. Experiment was performed in $CDCl_3$ at 298 K (400 MHz). (ϕ) $CHCl_3$, (*) H grease, (γ) TMS.

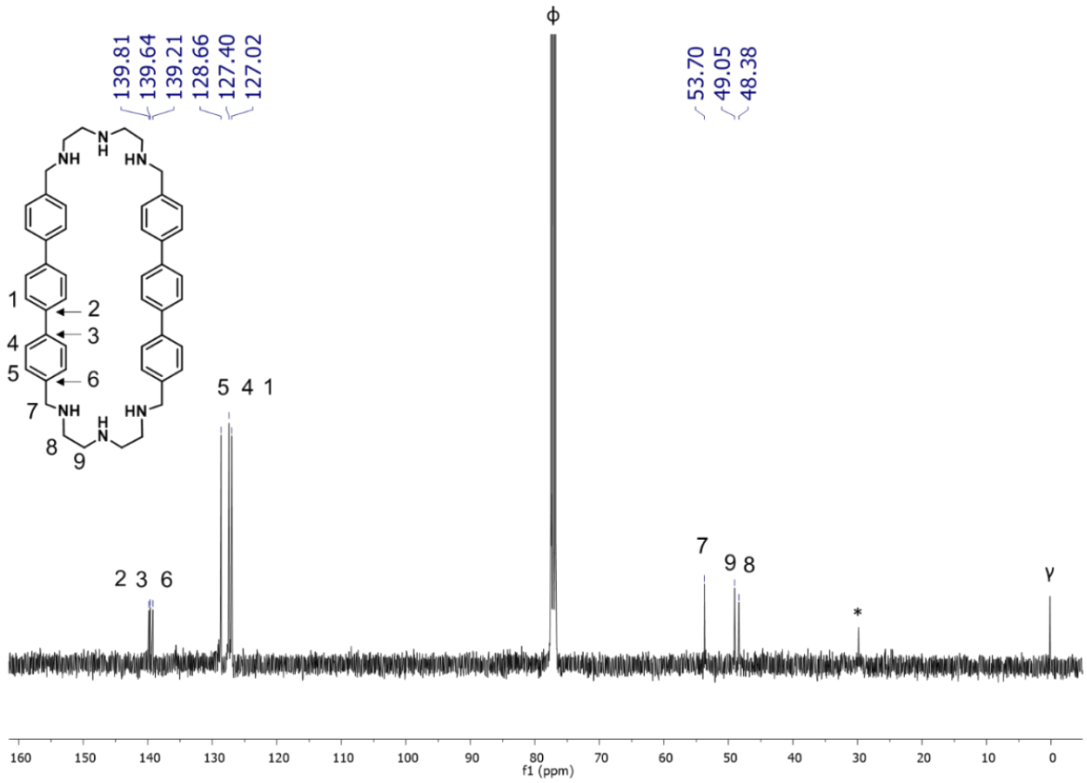

Supplementary Figure 38. ^{13}C-NMR of H_2ppp macrocycle. Experiment was performed in $CDCl_3$ at 298 K (100 MHz). (ϕ) $CHCl_3$, (*) H grease, (γ) TMS.

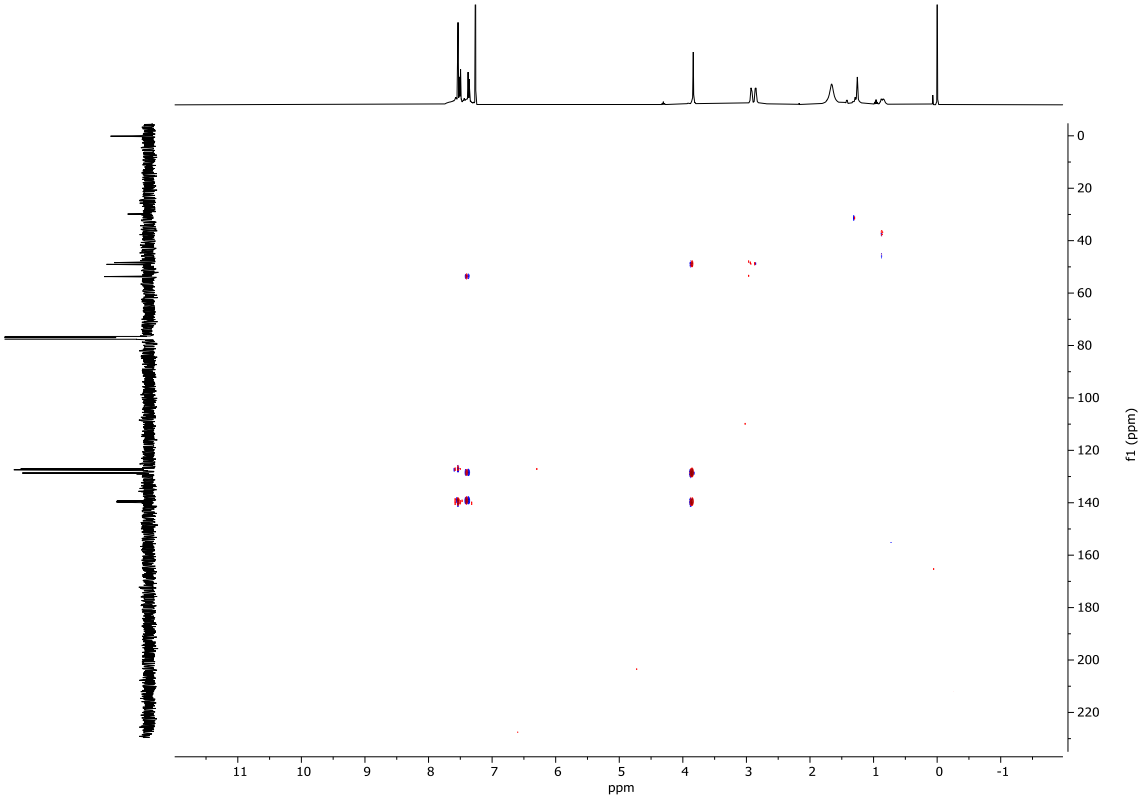

Supplementary Figure 39. HMBC of H_2ppp macrocycle. Experiment was performed in $CDCl_3$ at 298 K (400 MHz).

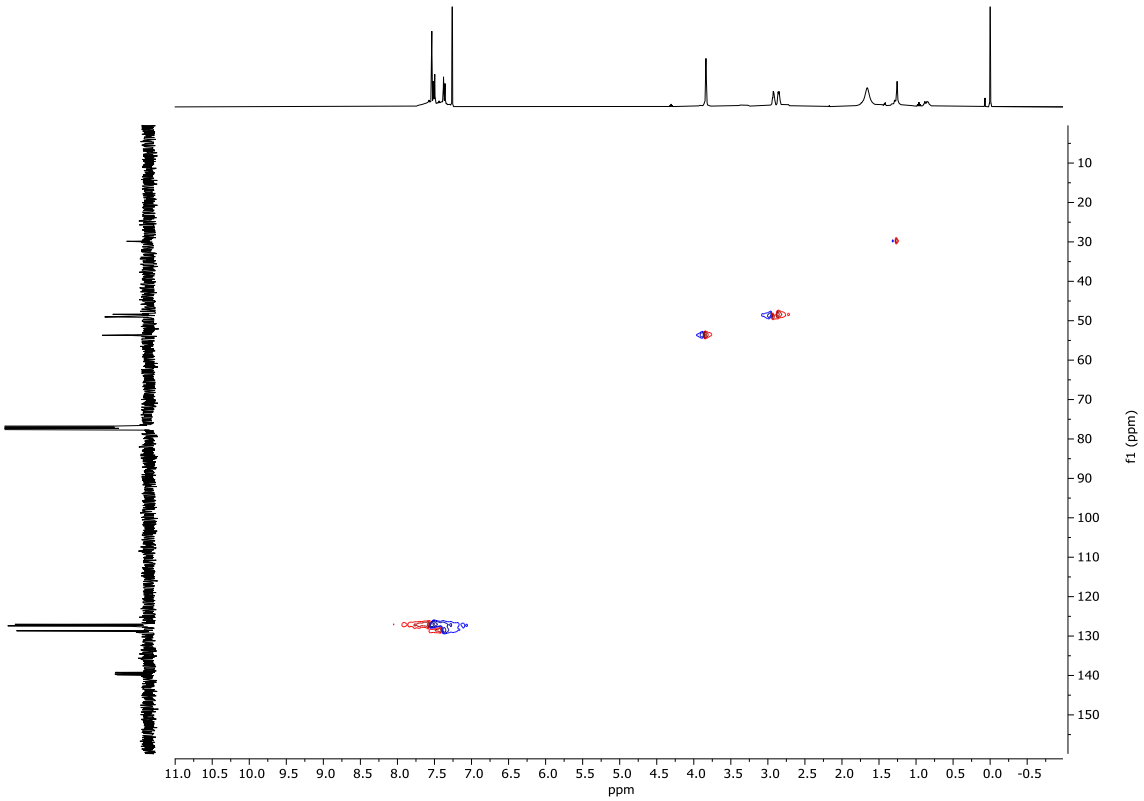

Supplementary Figure 40. HSQC of H_2ppp macrocycle. Experiment was performed in $CDCl_3$ at 298 K (400 MHz).

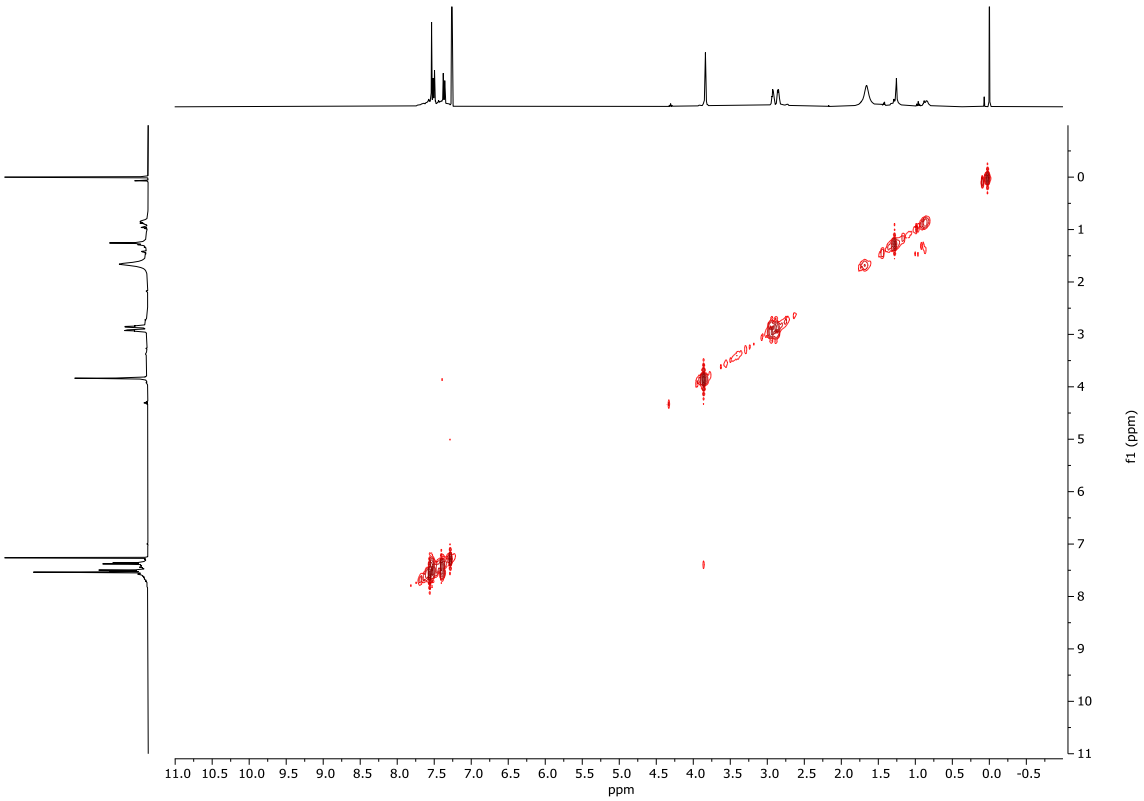

Supplementary Figure 41. COSY of H_2ppp macrocycle. Experiment was performed in $CDCl_3$ at 298 K (400 MHz).

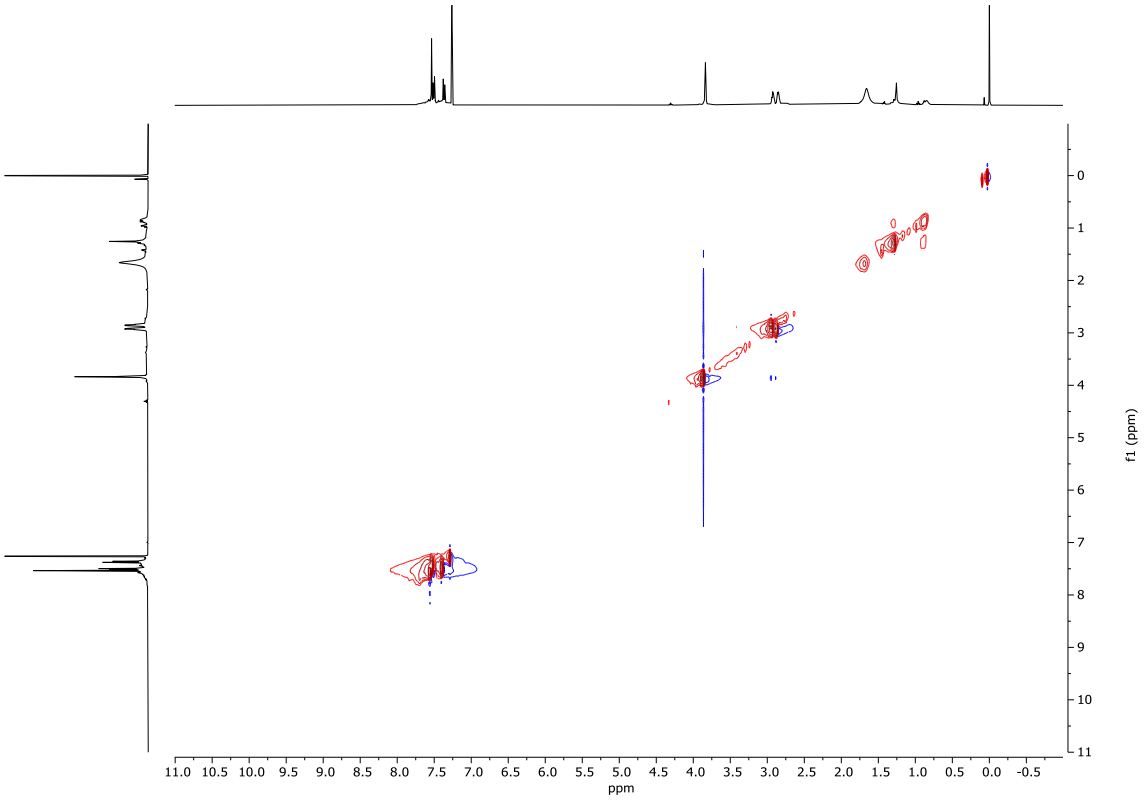

Supplementary Figure 42. TOCSY of H_2ppp macrocycle. Experiment was performed in $CDCl_3$ at 298 K (400 MHz).

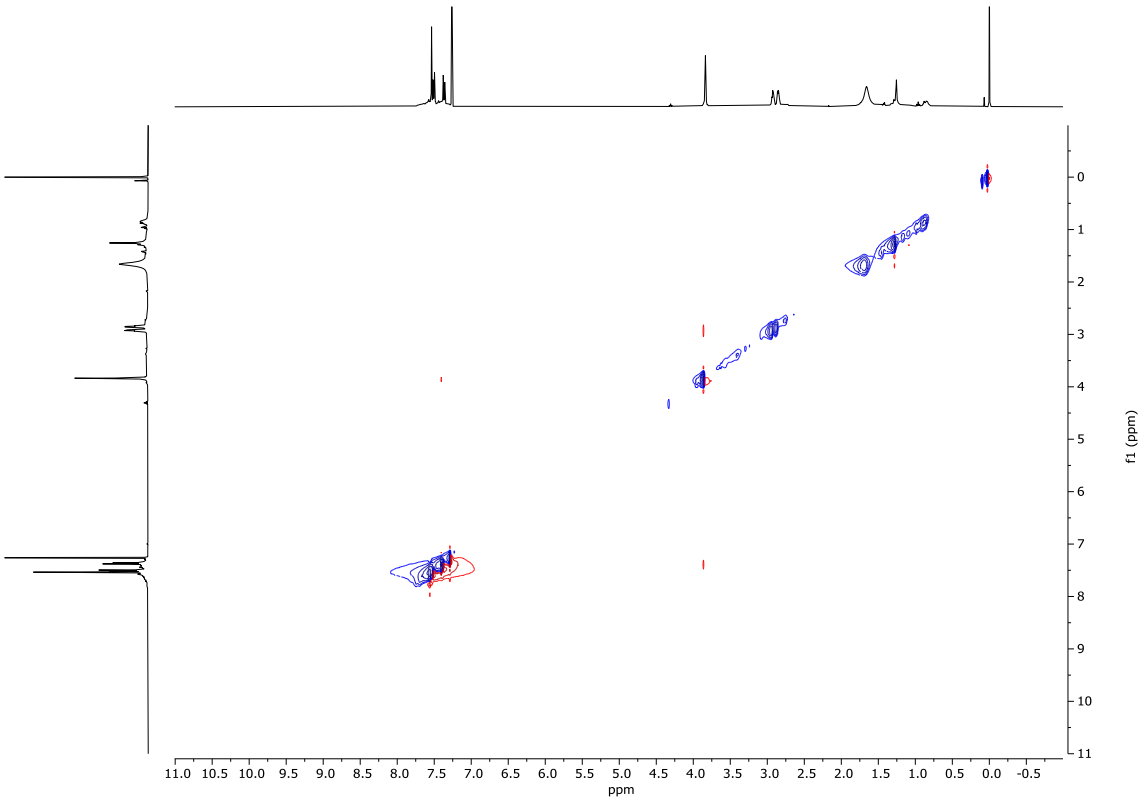

Supplementary Figure 43. NOESY of H_2ppp macrocycle. Experiment was performed in $CDCl_3$ at 298 K (400 MHz).

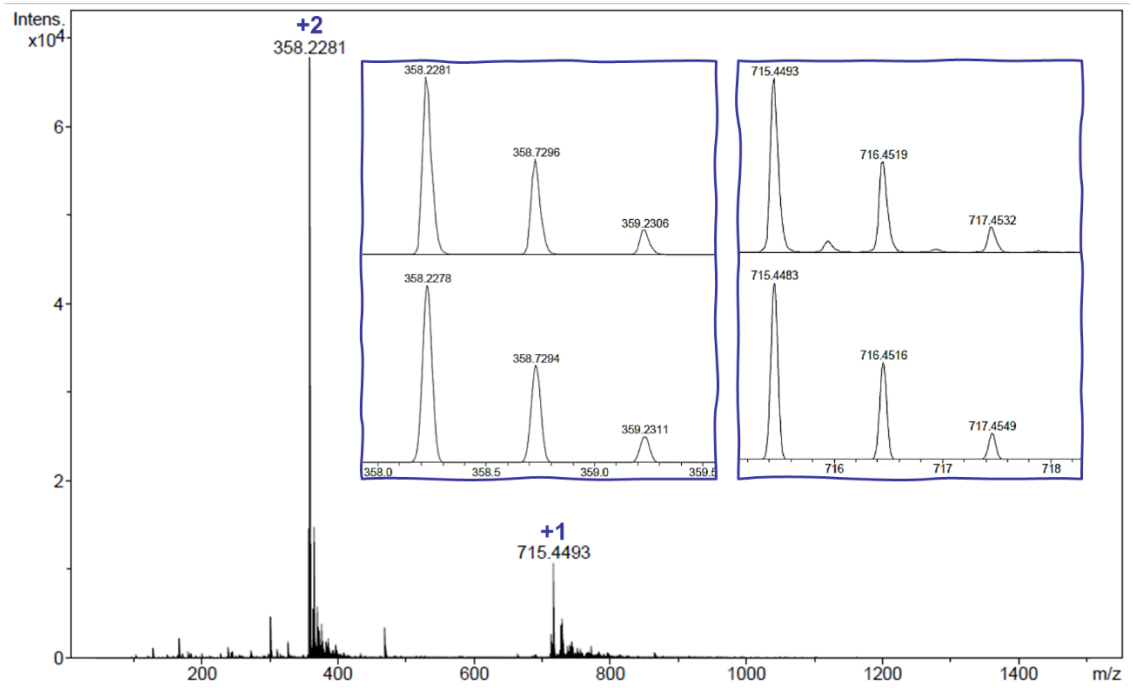

Supplementary Figure 44. HRMS spectrum of H_2ppp macrocycle. Experimental (top) and theoretical (bottom) isotopic pattern for selected peaks is shown. The sample was dissolved in chloroform and the spectrum was registered on a Bruker Micro TOF-Q-II exact mass spectrometer.

2.4. Characterization of the macrocyclic ligand Me_2ppp

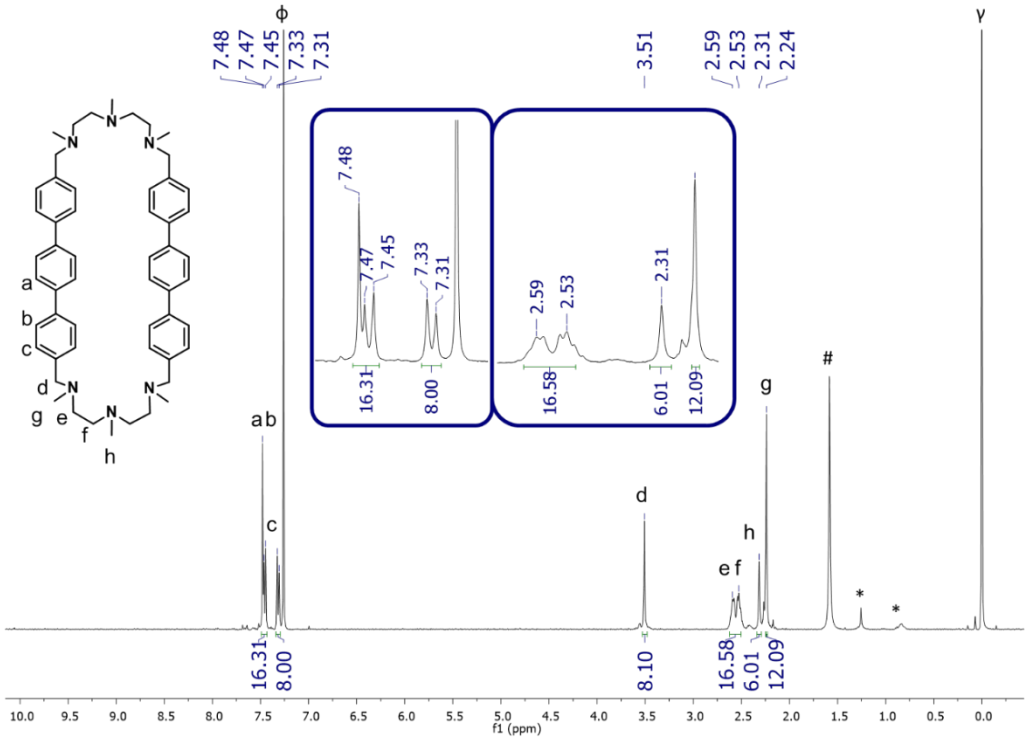

Supplementary Figure 45. ^{1}H-NMR of Me_2ppp macrocycle. Experiment was performed in $CDCl_3$ at 298 K (400 MHz). (#) H_2O, (*) H grease, (γ) TMS.

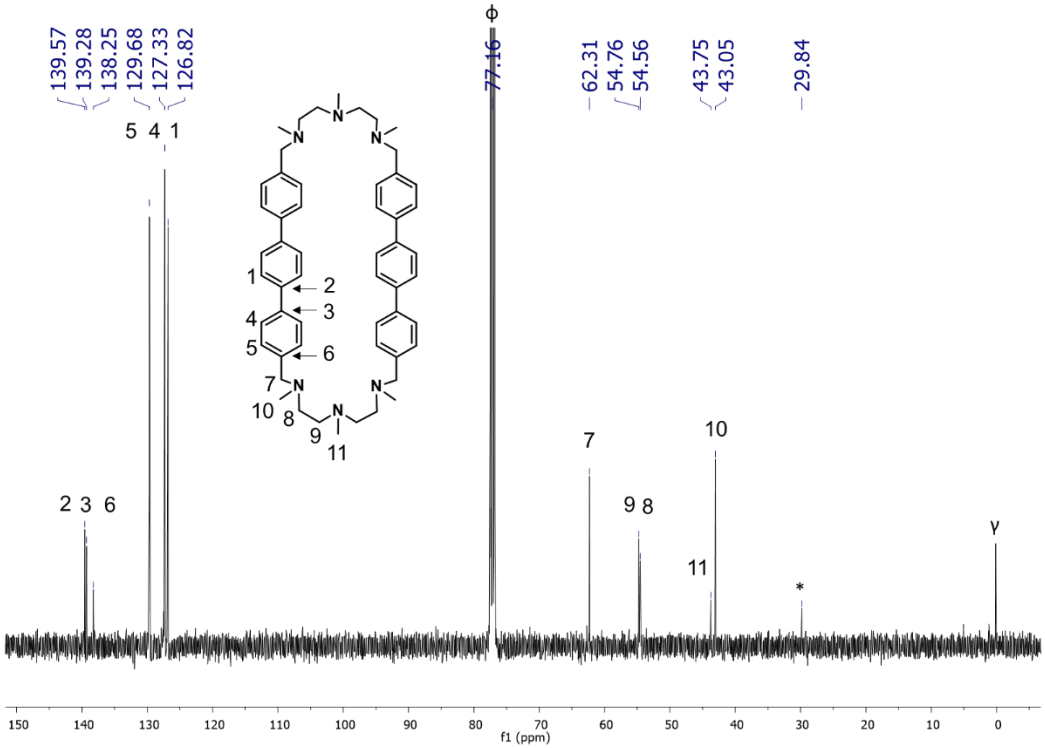

Supplementary Figure 46. ^{13}C-NMR of Me_2ppp macrocycle. Experiment was performed in $CDCl_3$ at 298 K (100 MHz). (ϕ) $CHCl_3$, (*) H grease, (γ) TMS.

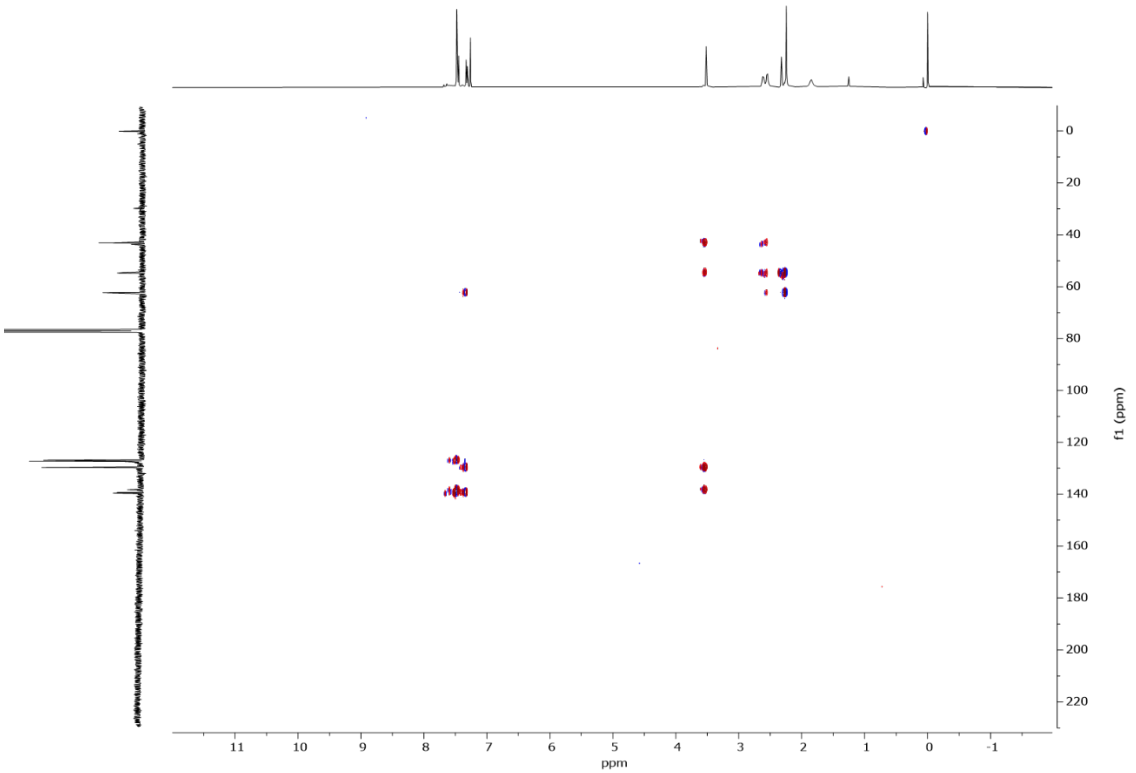

Supplementary Figure 47. HMBC of Me_2ppp macrocycle. Experiment was performed in $CDCl_3$ at 298 K (400 MHz).

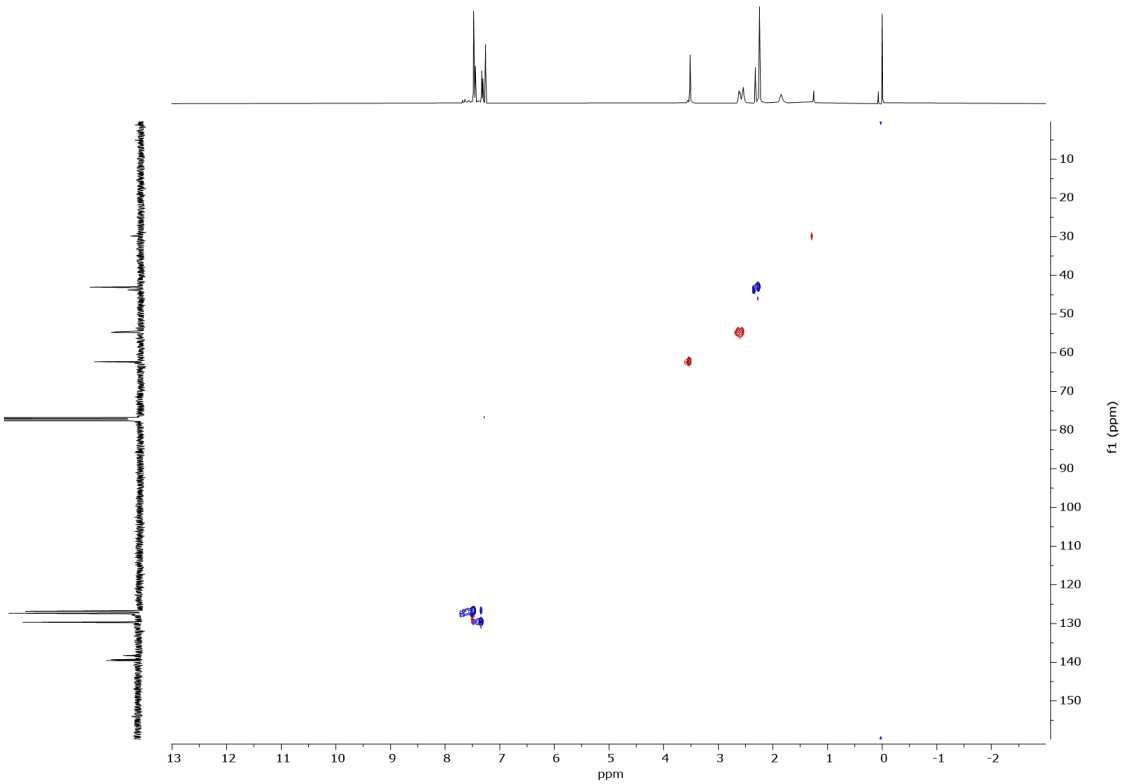

Supplementary Figure 48. HSQC of Me_2ppp macrocycle. Experiment was performed in $CDCl_3$ at 298 K (400 MHz).

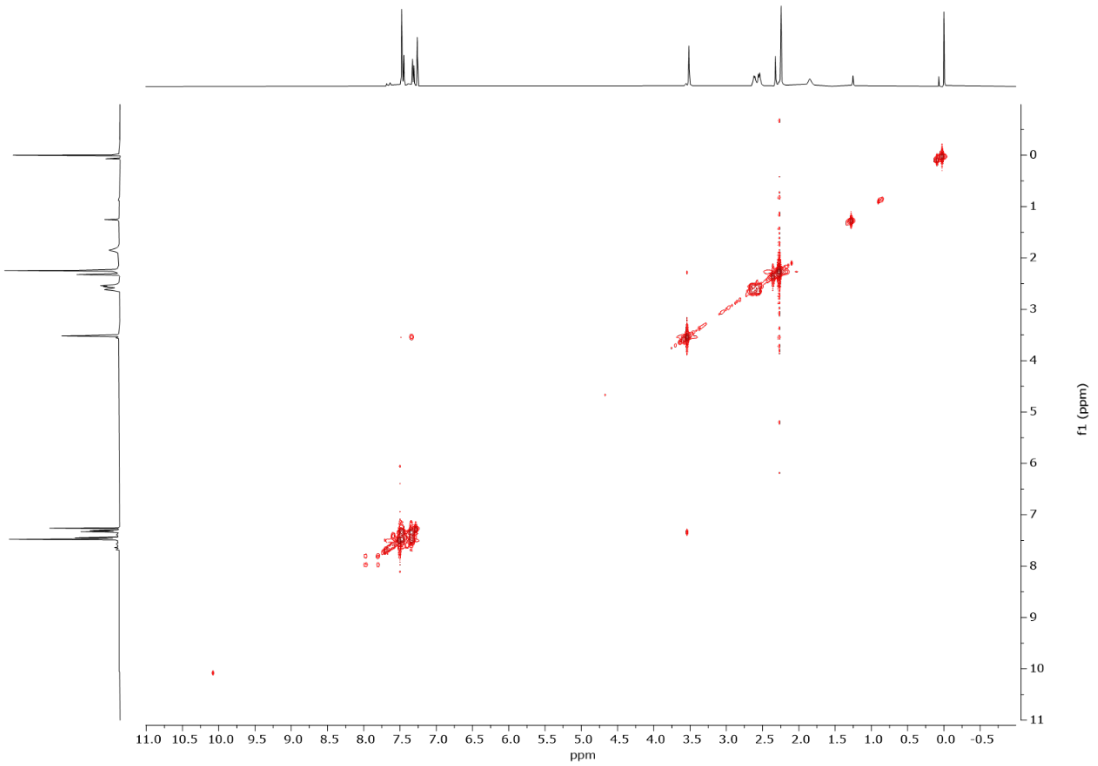

Supplementary Figure 49. COSY of Me_2ppp macrocycle. Experiment was performed in $CDCl_3$ at 298 K (400 MHz).

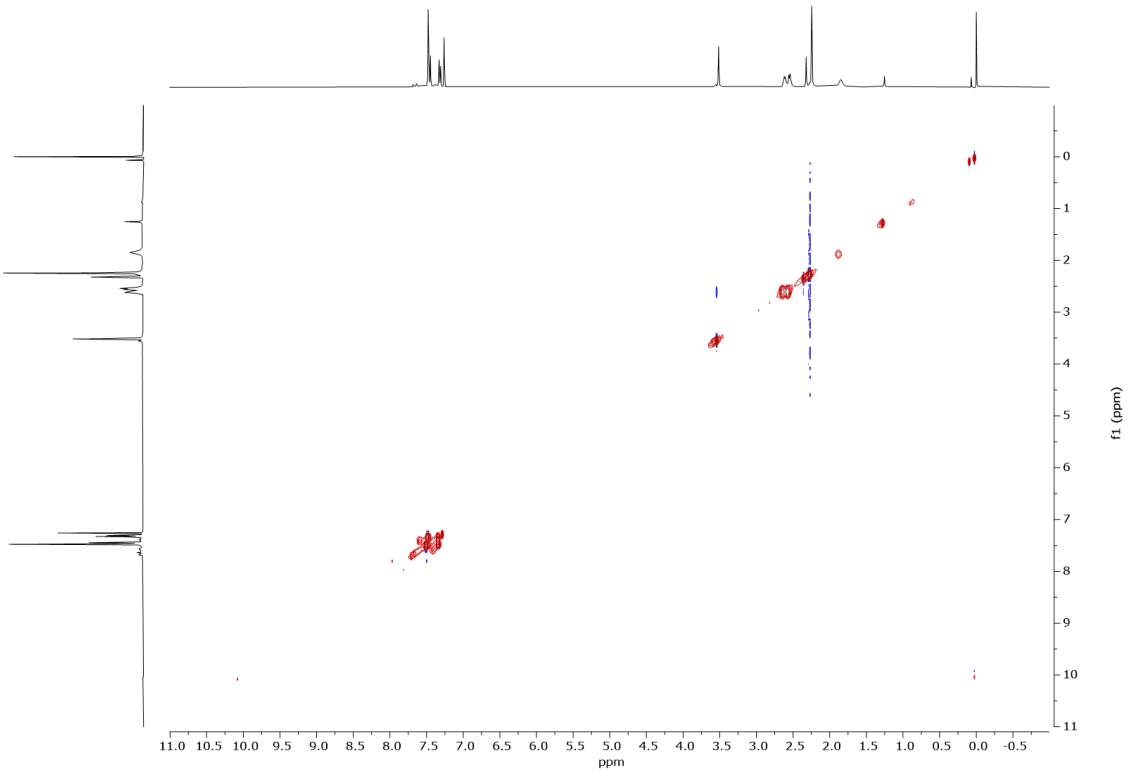

Supplementary Figure 50. TOCSY of Me_2ppp macrocycle. Experiment was performed in $CDCl_3$ at 298 K (400 MHz).

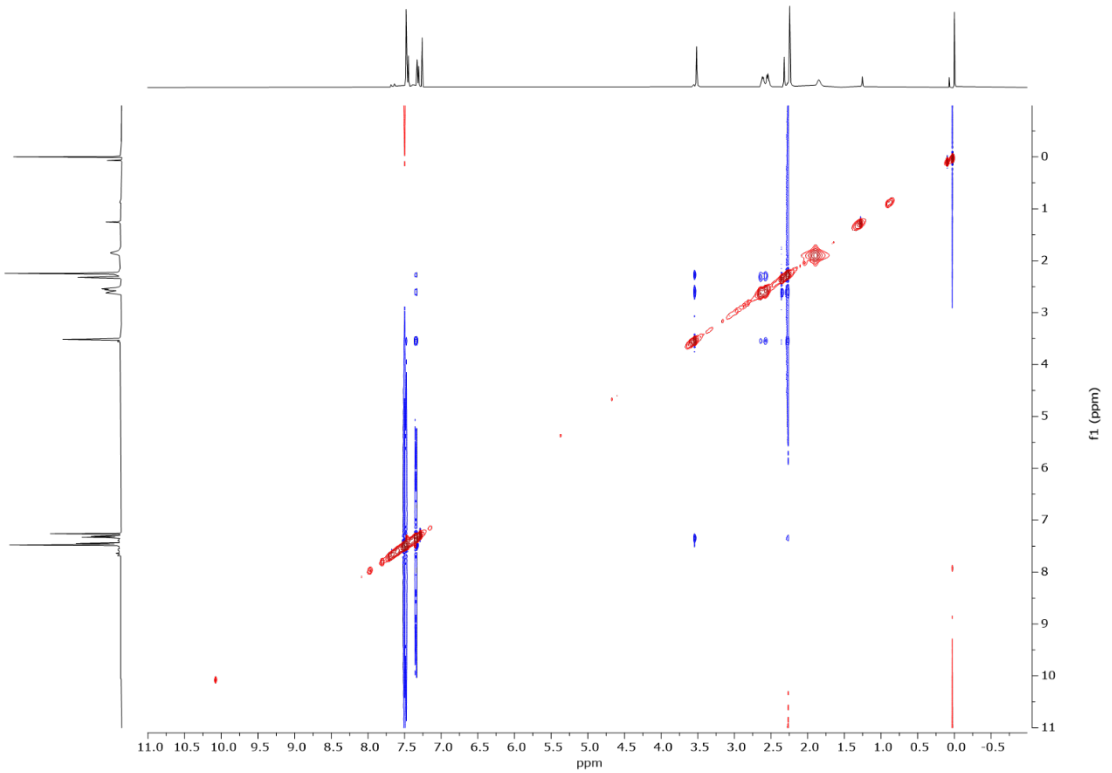

Supplementary Figure 51. NOESY of Me_2ppp macrocycle. Experiment was performed in $CDCl_3$ at 298 K (400 MHz).

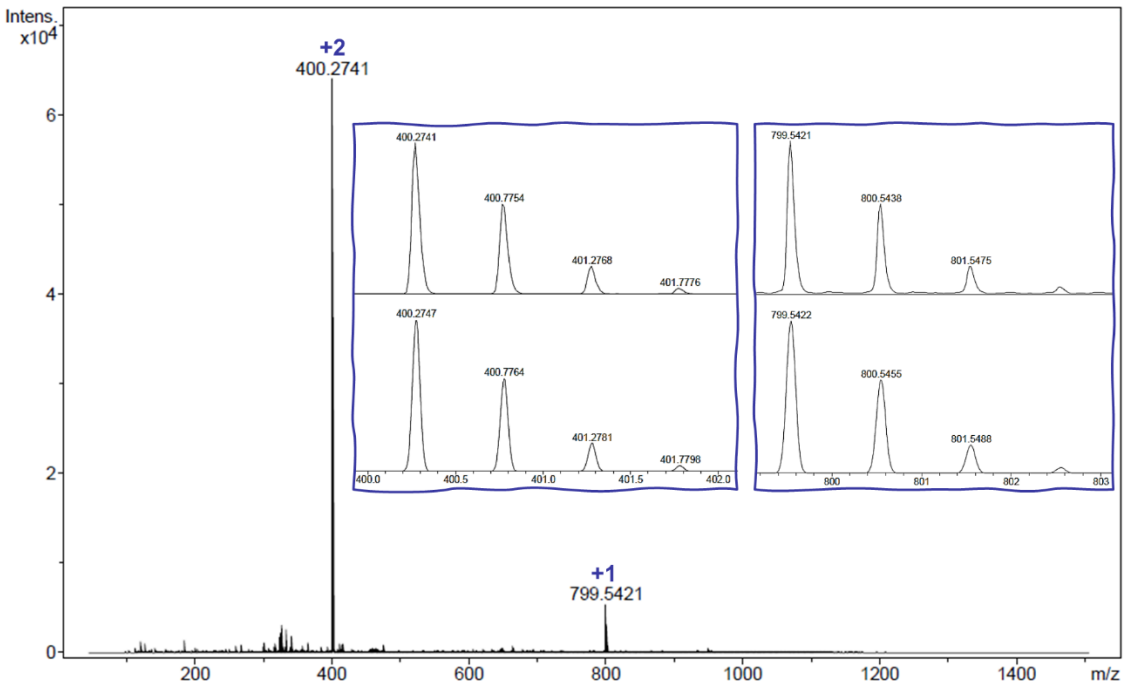

Supplementary Figure 52. HRMS spectrum of Me_2ppp macrocycle. Experimental (top) and theoretical (bottom) isotopic pattern for selected peaks is shown. The sample was dissolved in chloroform and the spectrum was registered on a Bruker Micro TOF-Q-II exact mass spectrometer.

2.5. Characterization of dinuclear Pd^{II} molecular clip [Pd_2-$Me_2ppp{\cdot}(AcO)_2(OTf)_2$]

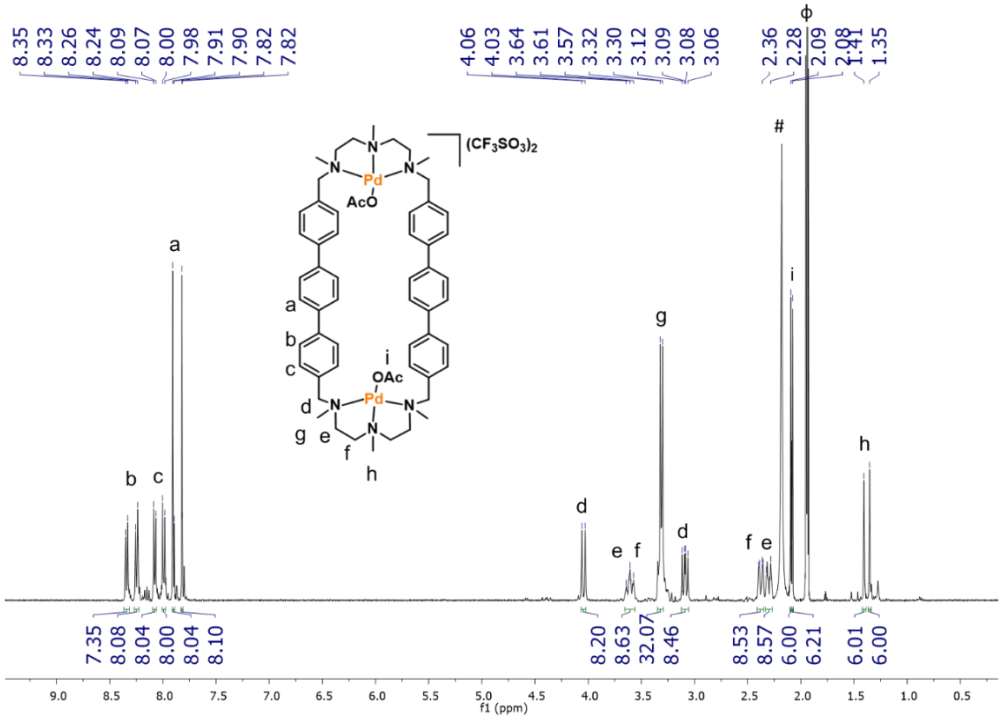

Supplementary Figure 53. ^{1}H-NMR of $[Pd_2(Me_2ppp)(AcO)_2](OTf)_2$. Experiment was performed in CD_3CN at 298 K (400 MHz). (ϕ) CH_3CN, (#) H_2O.

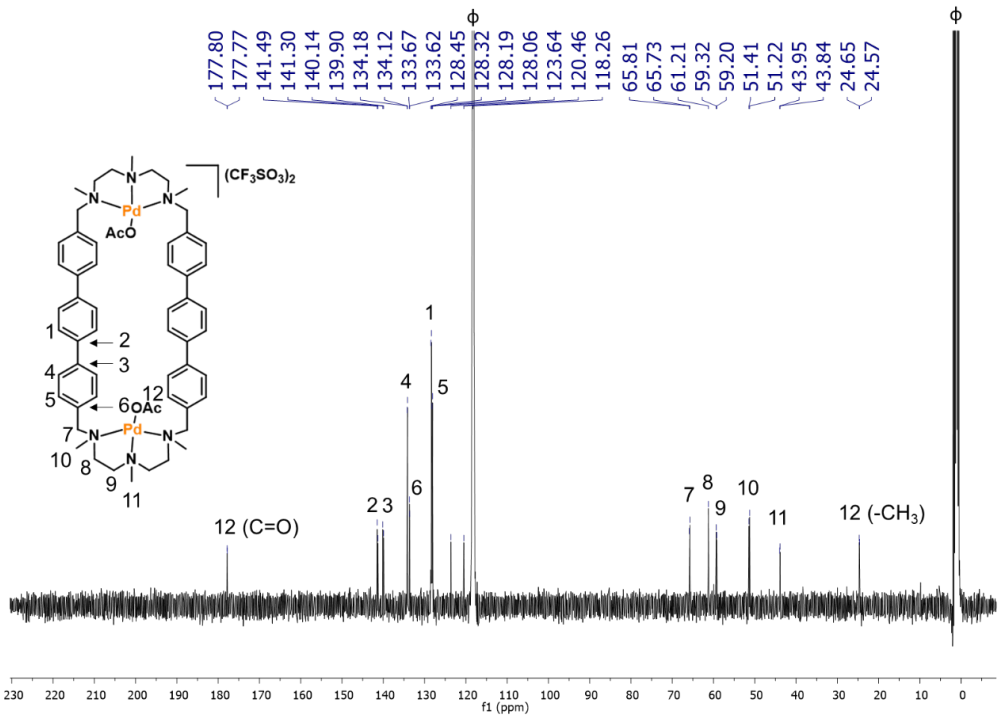

Supplementary Figure 54. ^{13}C-NMR of $[Pd_2(Me_2ppp)(AcO)_2](OTf)_2$. Experiment was performed in CD_3CN at 298 K (100 MHz). (ϕ) CH_3CN.

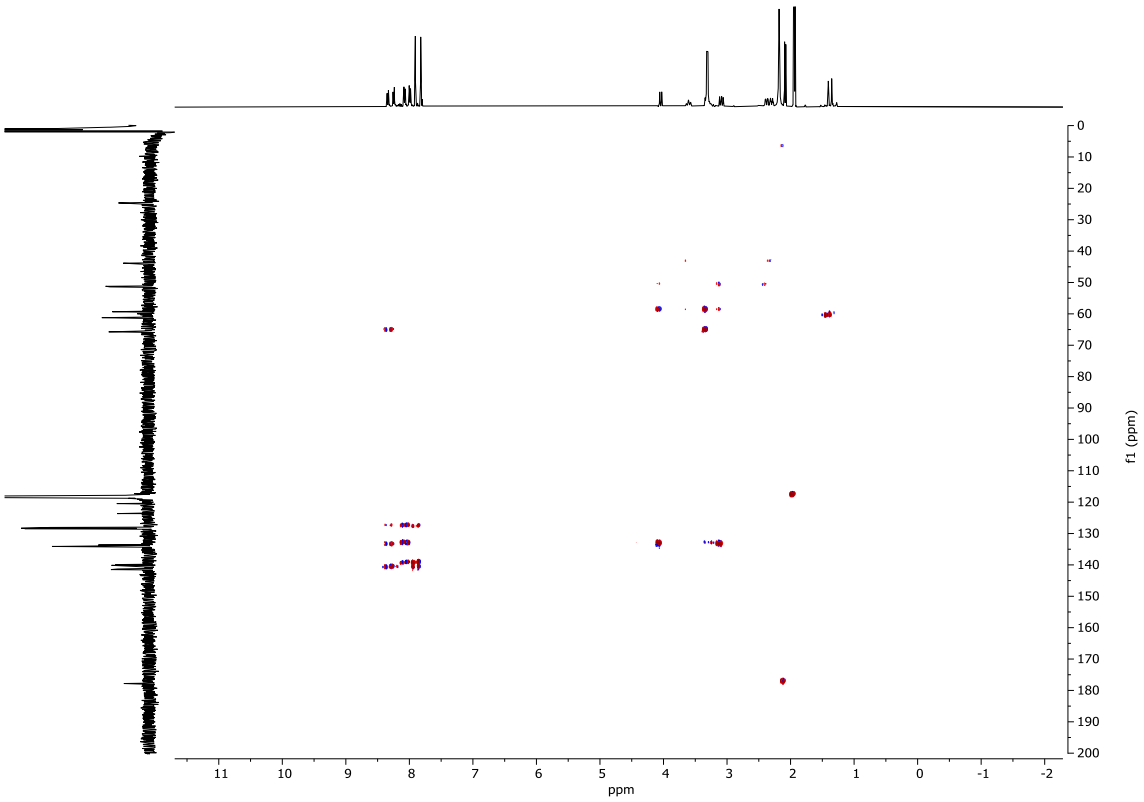

Supplementary Figure 55. HMBC of $[Pd_2(Me_2ppp)(AcO)_2](OTf)_2$. Experiment was performed in CD_3CN at 298 K (400 MHz).

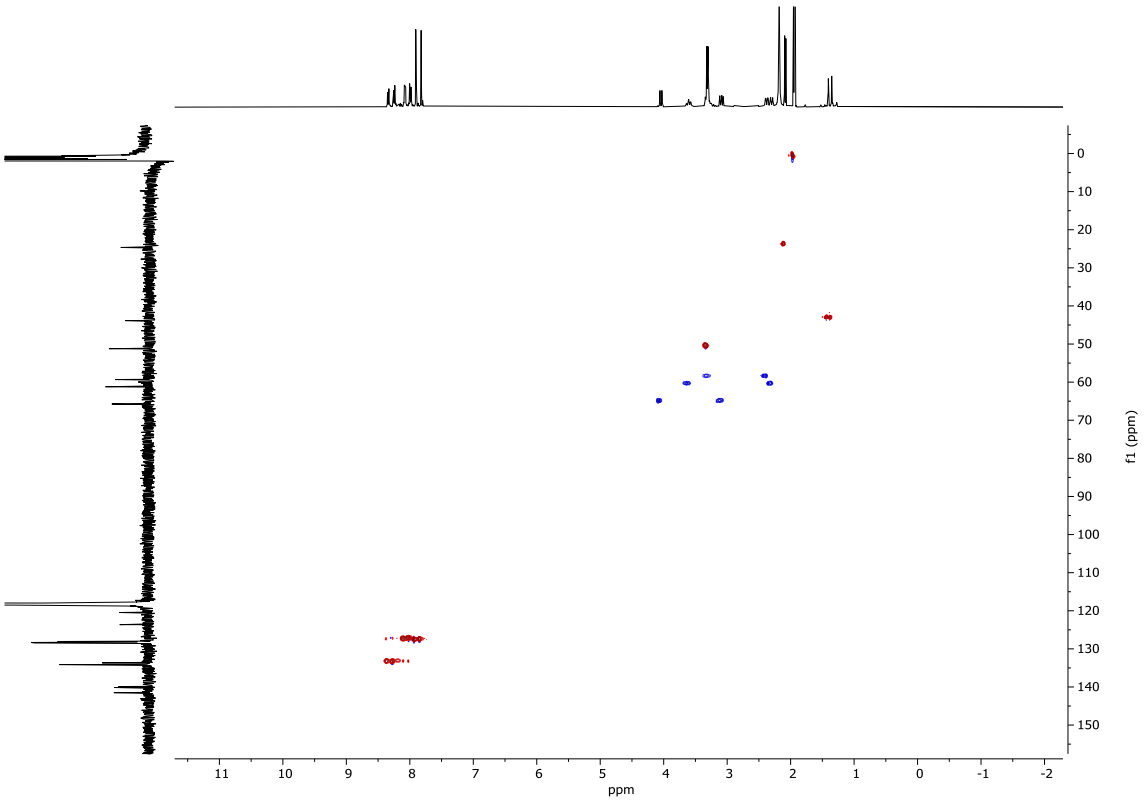

Supplementary Figure 56. HSQC of $[Pd_2(Me_2ppp)(AcO)_2](OTf)_2$. Experiment was performed in CD_3CN at 298 K (400 MHz).

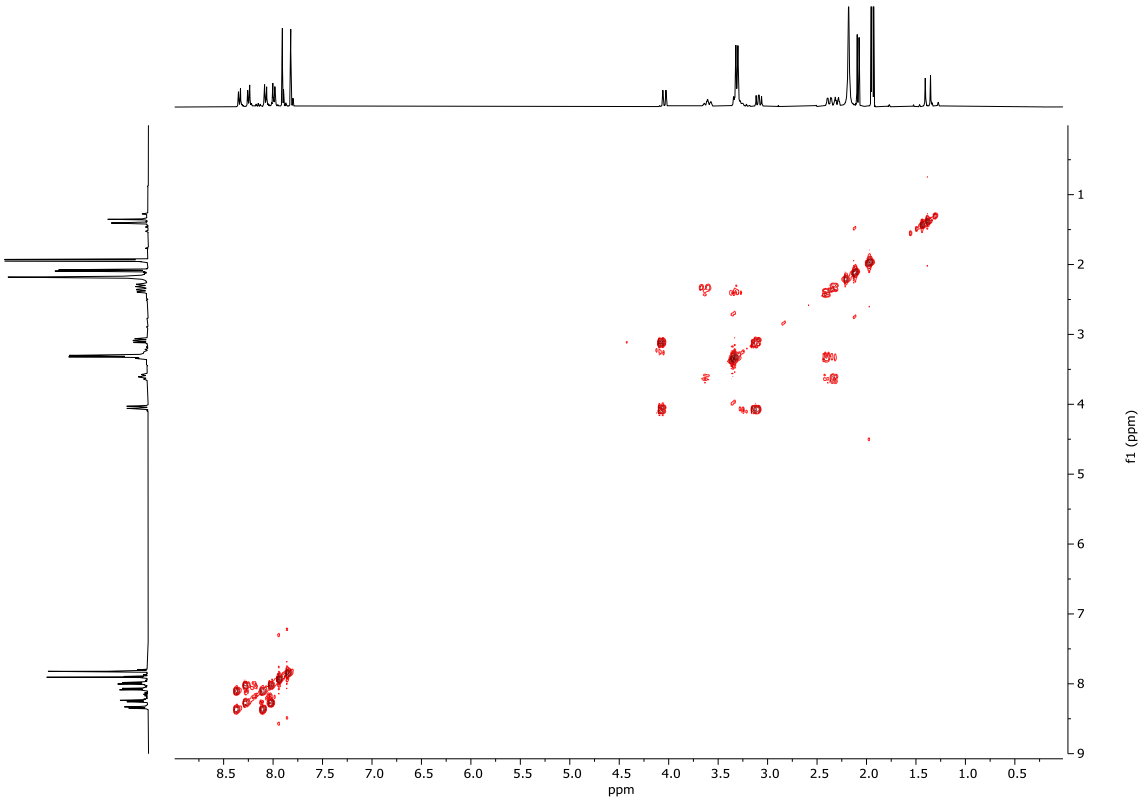

Supplementary Figure 57. COSY of $[Pd_2(Me_2ppp)(AcO)_2](OTf)_2$. Experiment was performed in CD_3CN at 298 K (400 MHz).

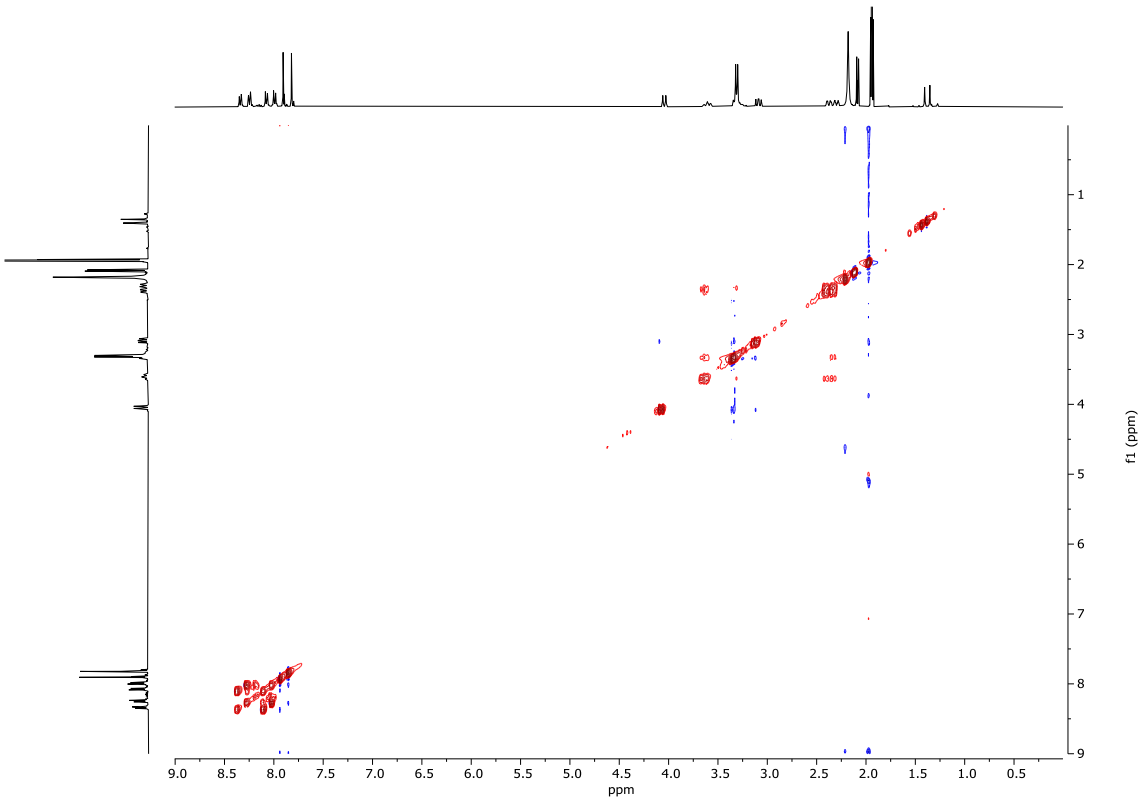

Supplementary Figure 58. TOCSY of $[Pd_2(Me_2ppp)(AcO)_2](OTf)_2$. Experiment was performed in CD_3CN at 298 K (400 MHz).

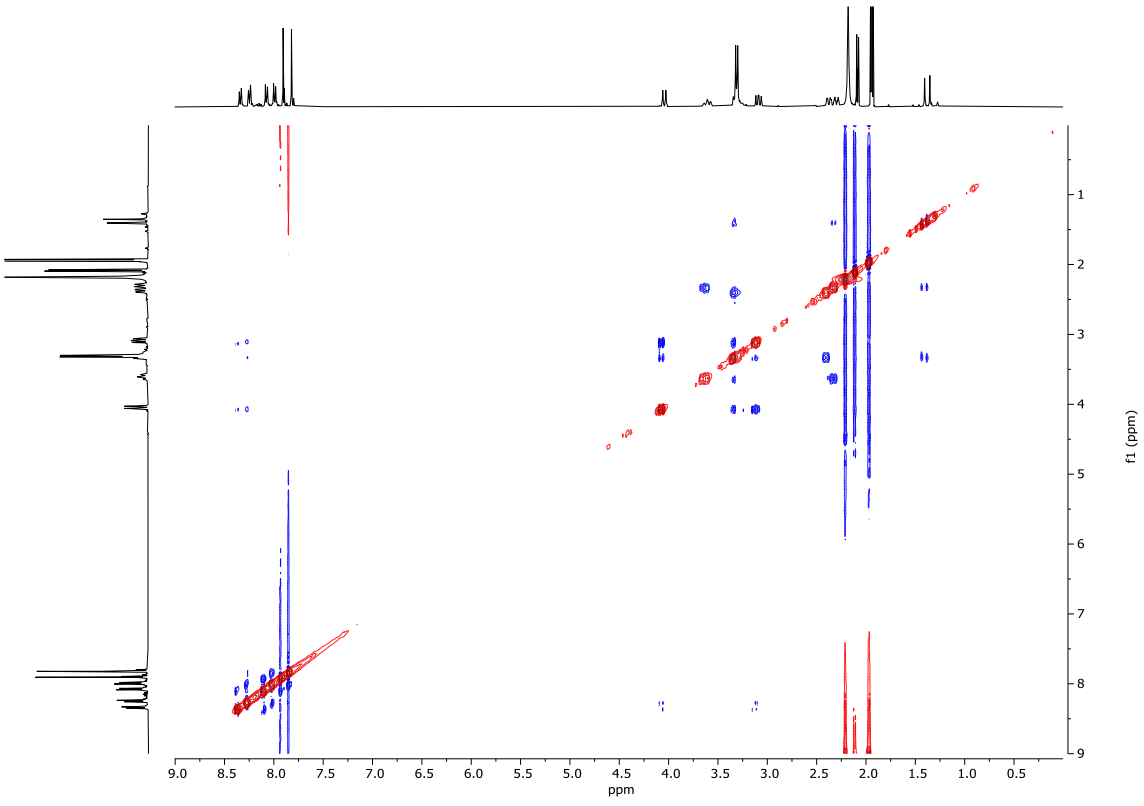

Supplementary Figure 59. NOESY of $[Pd_2(Me_2ppp)(AcO)_2](OTf)_2$. Experiment was performed in CD_3CN at 298 K (400 MHz).

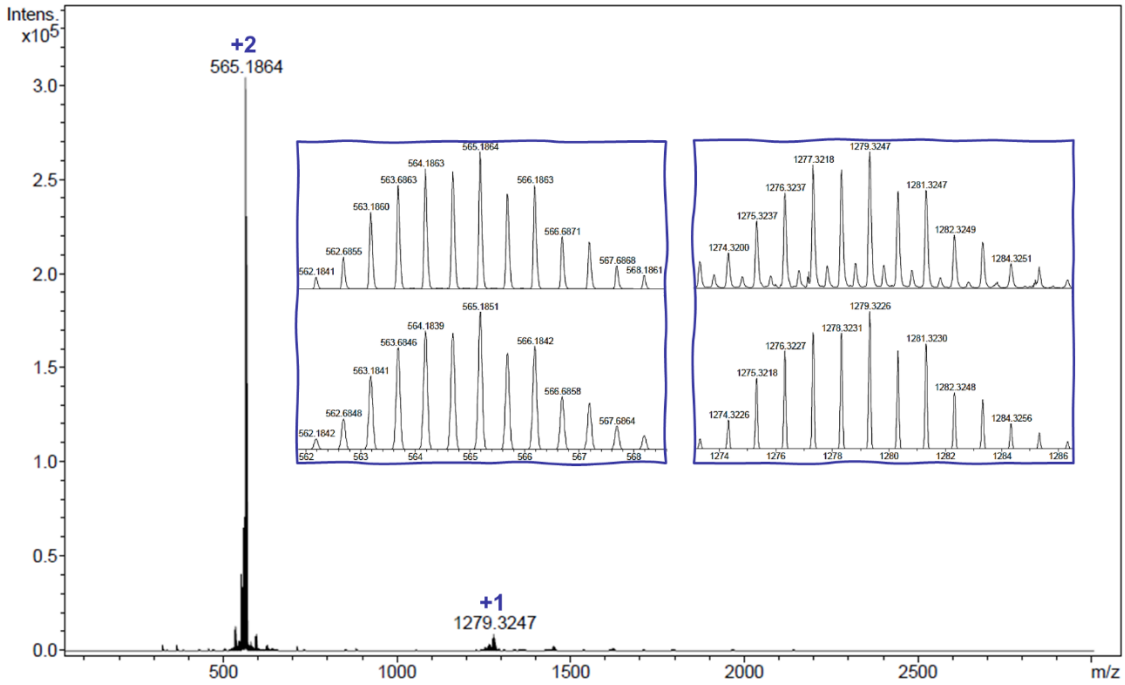

Supplementary Figure 60. HRMS spectrum of $[Pd_2(Me_2ppp)(AcO)_2](OTf)_2$. Experimental (top) and theoretical (bottom) isotopic pattern for selected peaks is shown. The sample was dissolved in acetonitrile and the spectrum was registered on a Bruker Micro TOF-Q-II exact mass spectrometer.

2.6. Characterization of dinuclear Cu^{II} molecular clip $[Cu_2(Me_2ppp)(OTf)_2](OTf)_2$

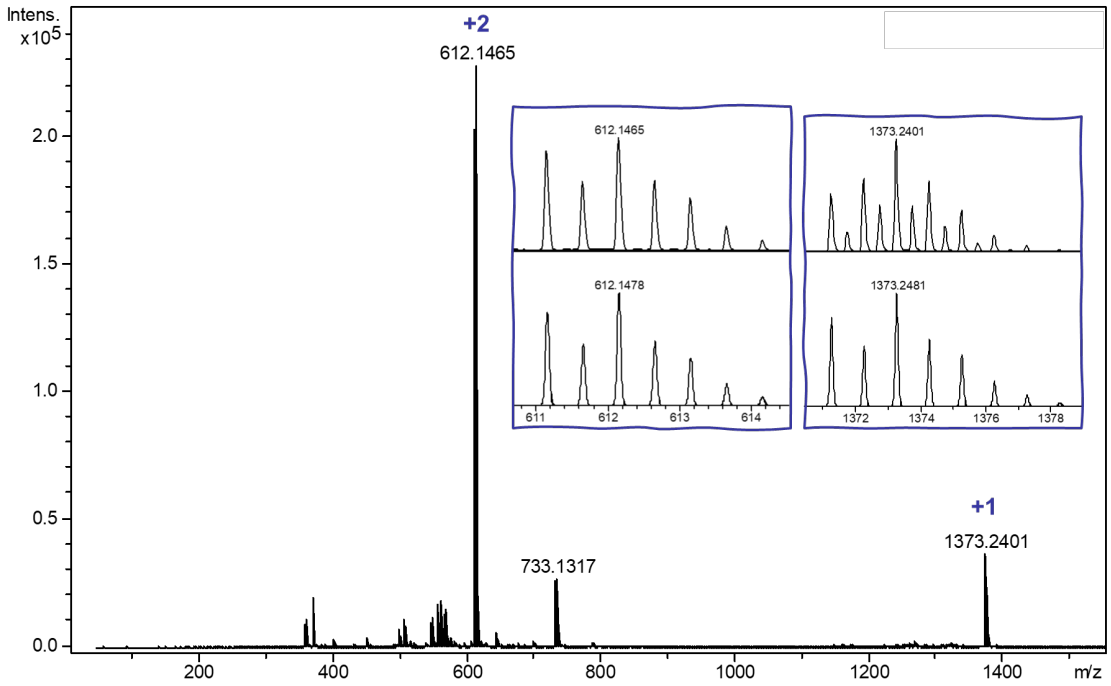

Supplementary Figure 61. HRMS spectrum of $[Cu_2(Me_2ppp)(OTf)_2](OTf)_2$. Experimental (top) and theoretical (bottom) isotopic pattern for selected peaks is shown. The sample was dissolved in acetonitrile and the spectrum was registered on a Bruker Micro TOF-Q-II exact mass spectrometer.

2.7. Characterization of tetragonal prismatic nanocapsule 8·(BArF)$_8$

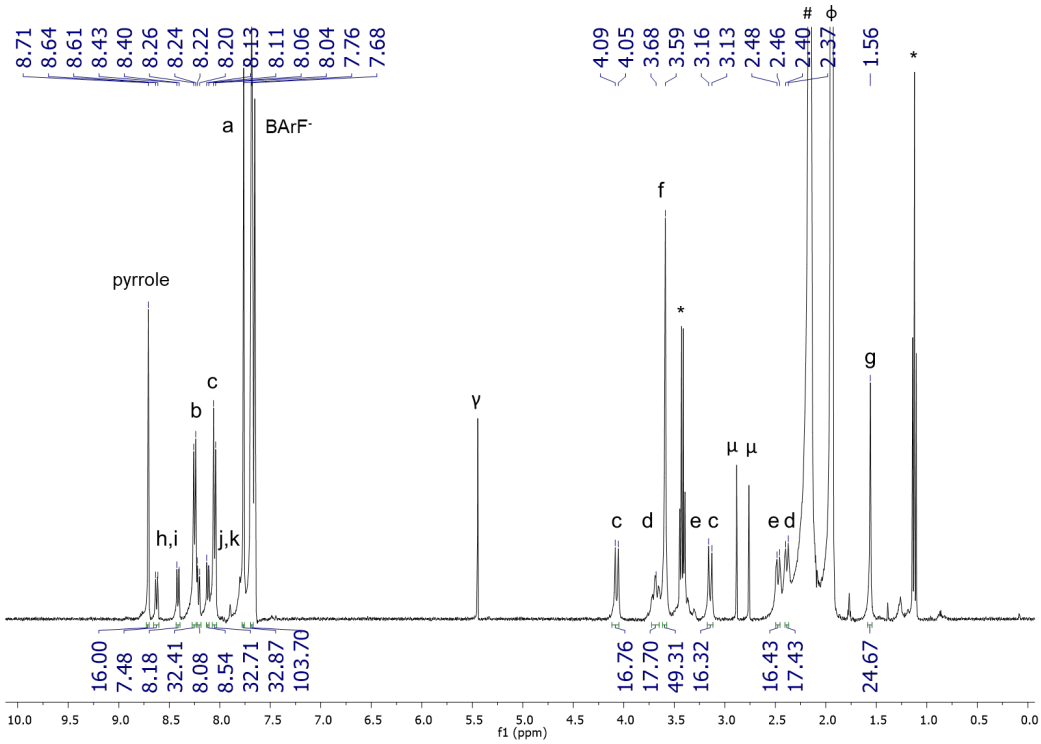

Supplementary Figure 62. ^{1}H-NMR of **8**·(BArF)$_8$ nanocapsule. Experiment was performed in CD_3CN at 298 K (400 MHz). (γ) DCM, (*) diethyl ether, (μ) dmf, (#) H_2O, (ϕ) CH_3CN.

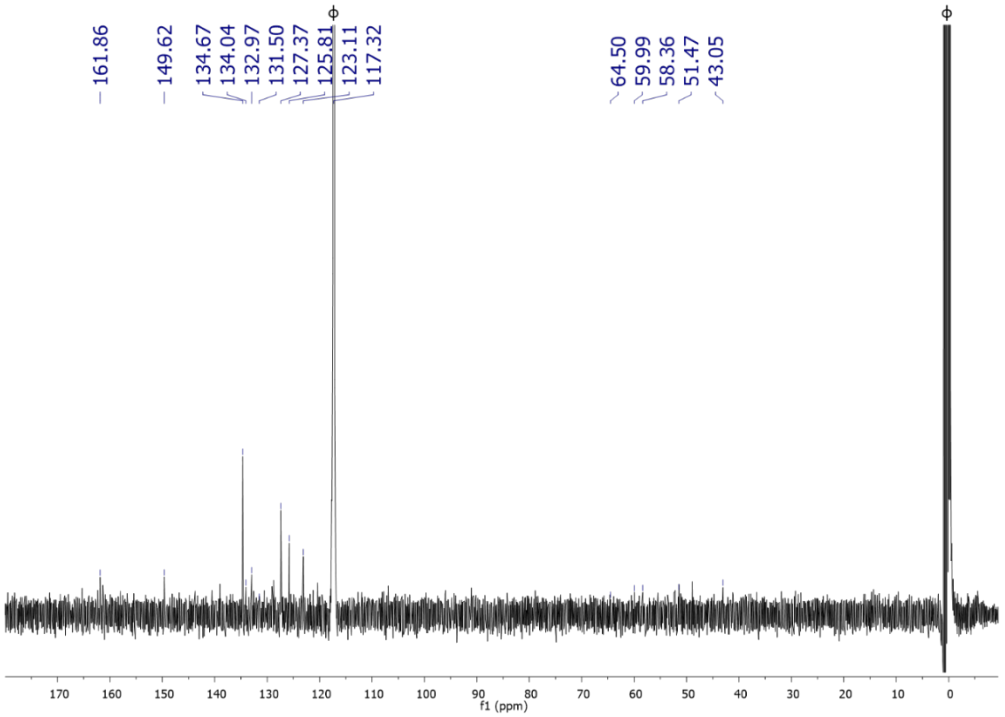

Supplementary Figure 63. ^{13}C-NMR of 8·$(BArF)_8$ nanocapsule. Experiment was performed in CD_3CN at 298 K (100 MHz). (ϕ) CH_3CN.

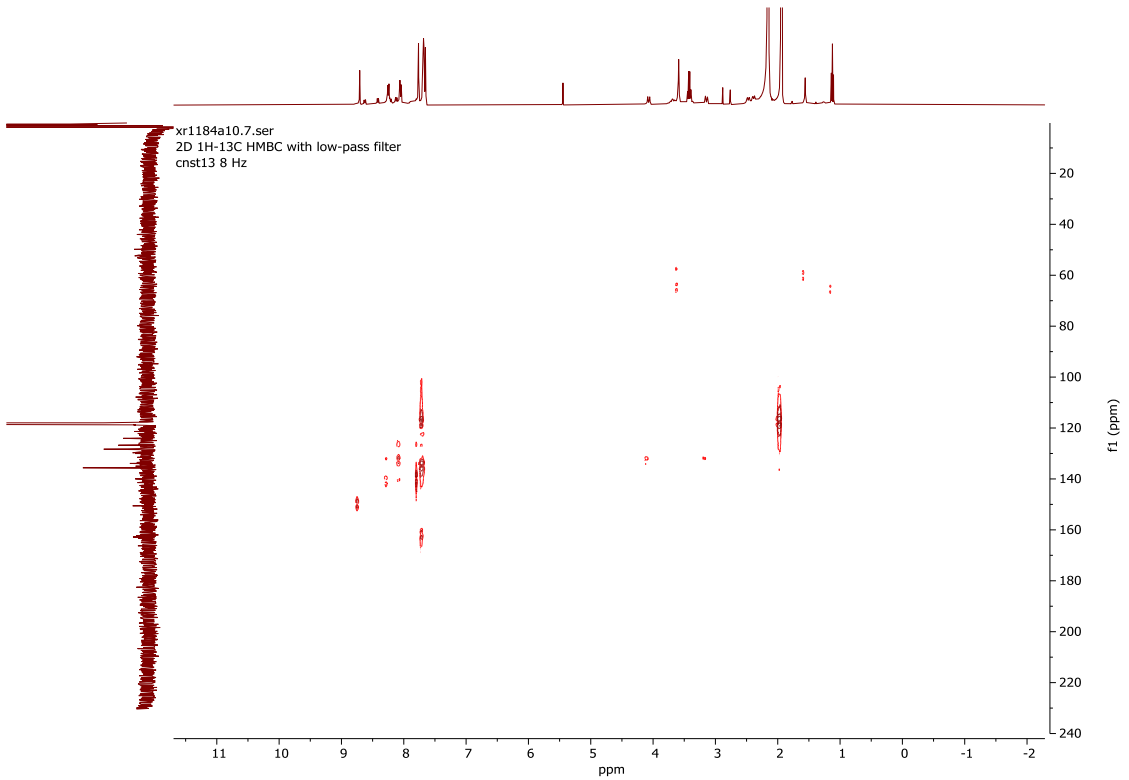

Supplementary Figure 64. HMBC of **8**·$(BArF)_8$ nanocapsule. Experiment was performed in CD_3CN at 298 K (400 MHz).

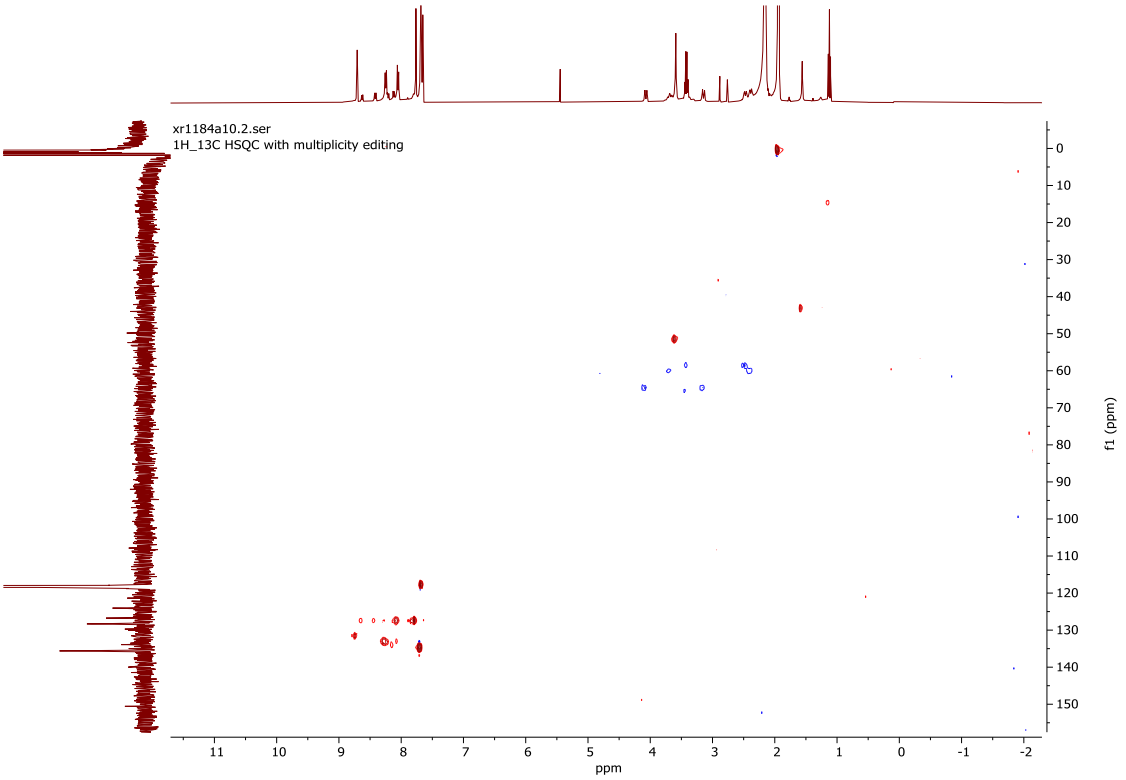

Supplementary Figure 65. HSQC of **8**·$(BArF)_8$ nanocapsule. Experiment was performed in CD_3CN at 298 K (400 MHz).

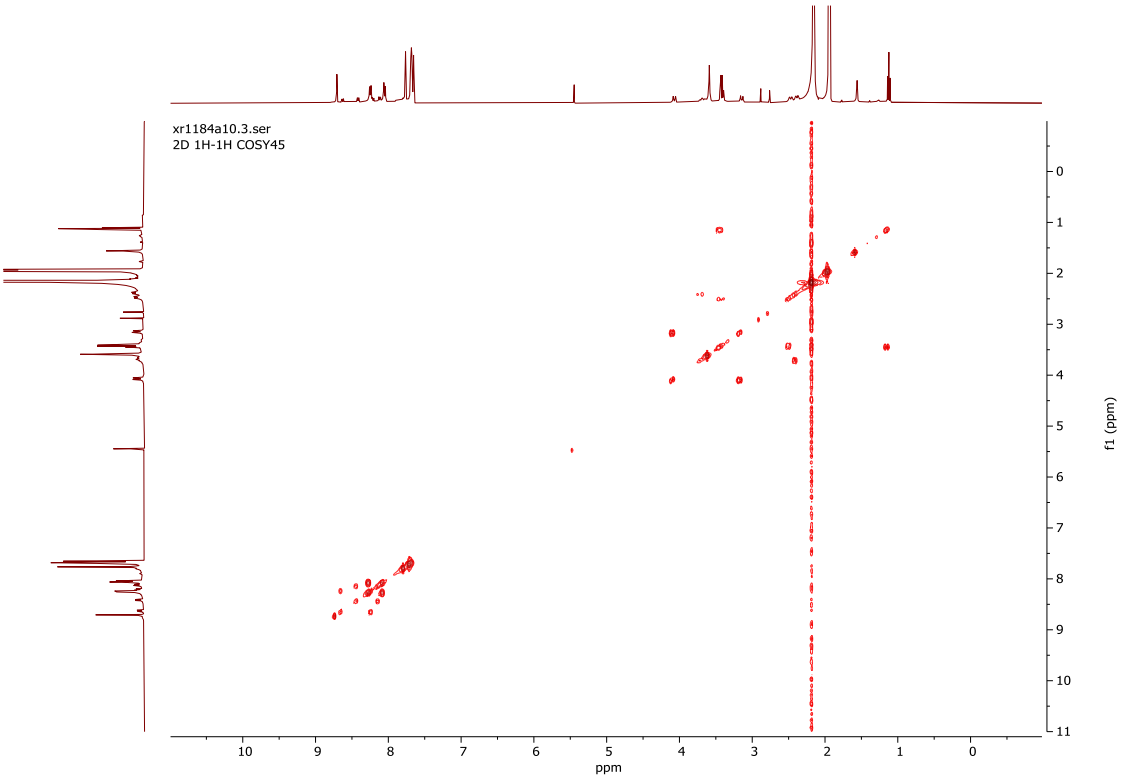

Supplementary Figure 66. COSY of **8**·$(BArF)_8$ nanocapsule. Experiment was performed in CD_3CN at 298 K (400 MHz).

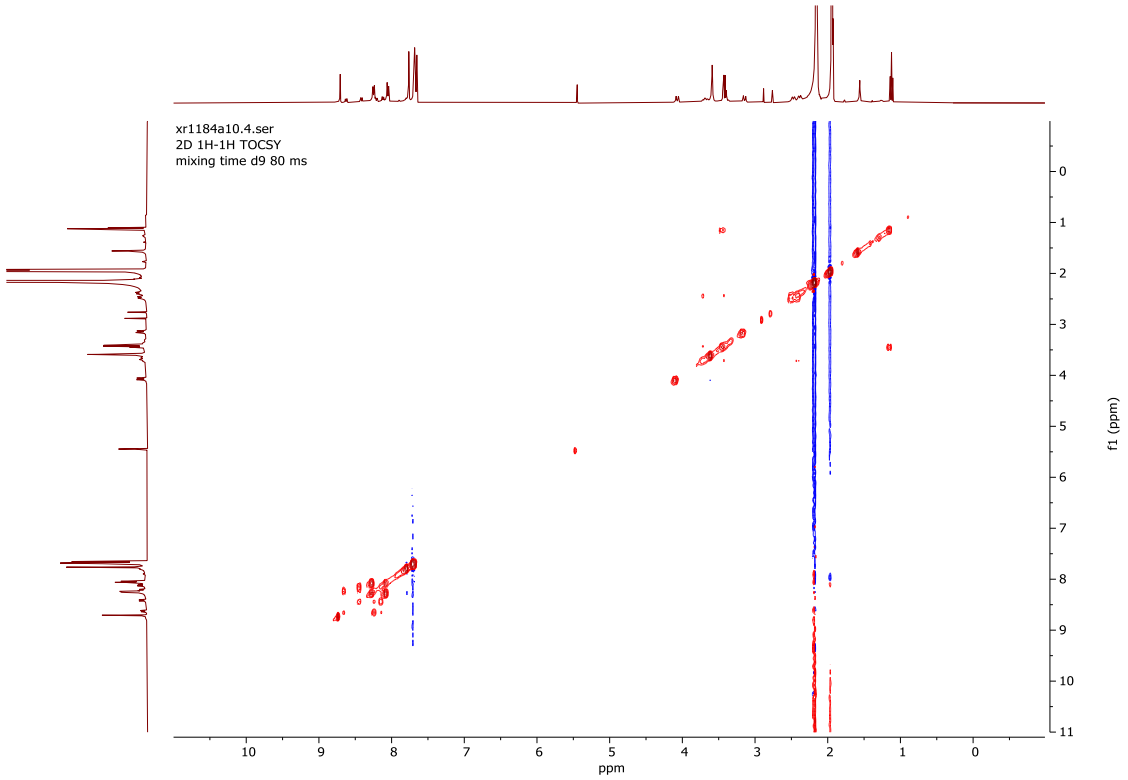

Supplementary Figure 67. TOCSY of **8**·$(BArF)_8$ nanocapsule. Experiment was performed in CD_3CN at 298 K (400 MHz).

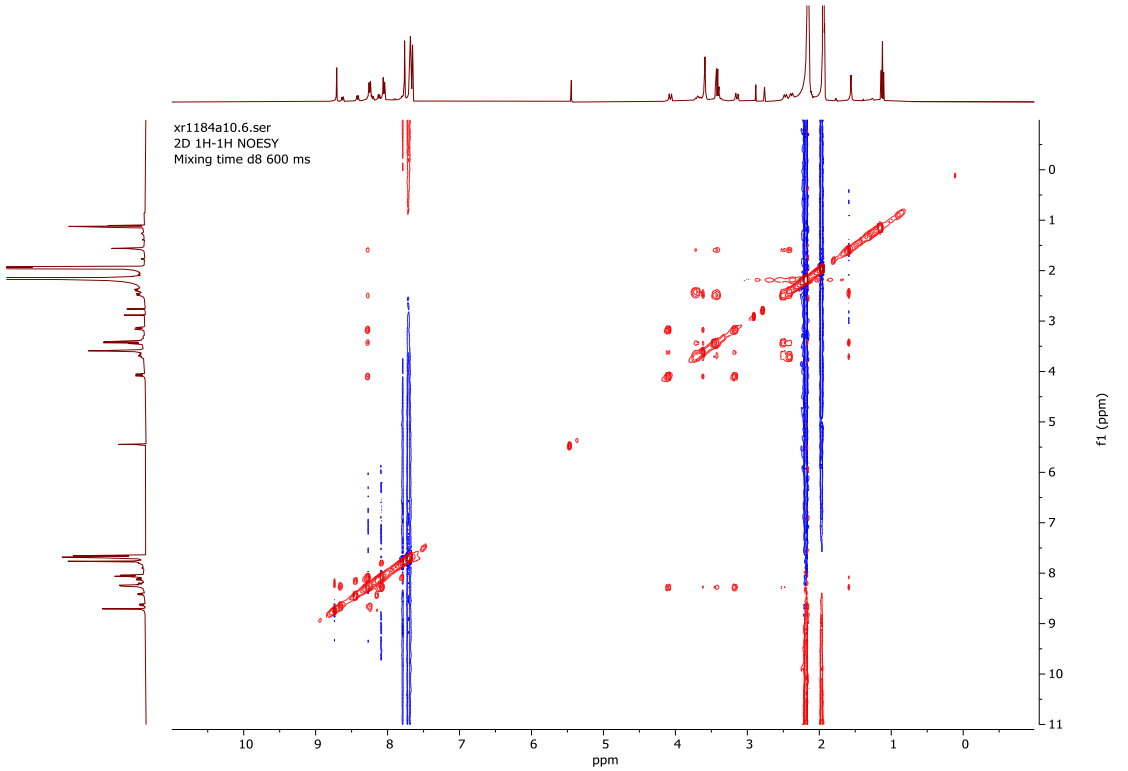

Supplementary Figure 68. NOESY of **8**·$(BArF)_8$ nanocapsule. Experiment was performed in CD_3CN at 298 K (400 MHz).

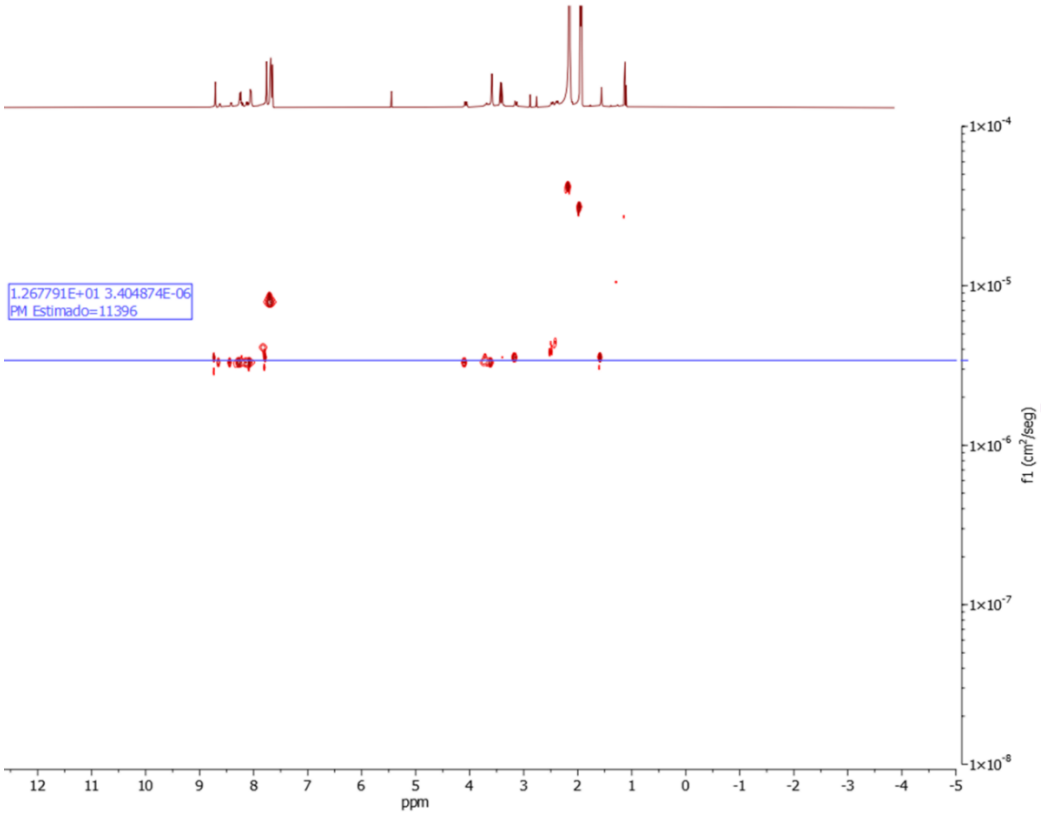

Supplementary Figure 69. DOSY of **8**·$(BArF)_8$ nanocapsule. Experiment was performed in CD_3CN at 298 K (400 MHz). (ф) CH_3CN.

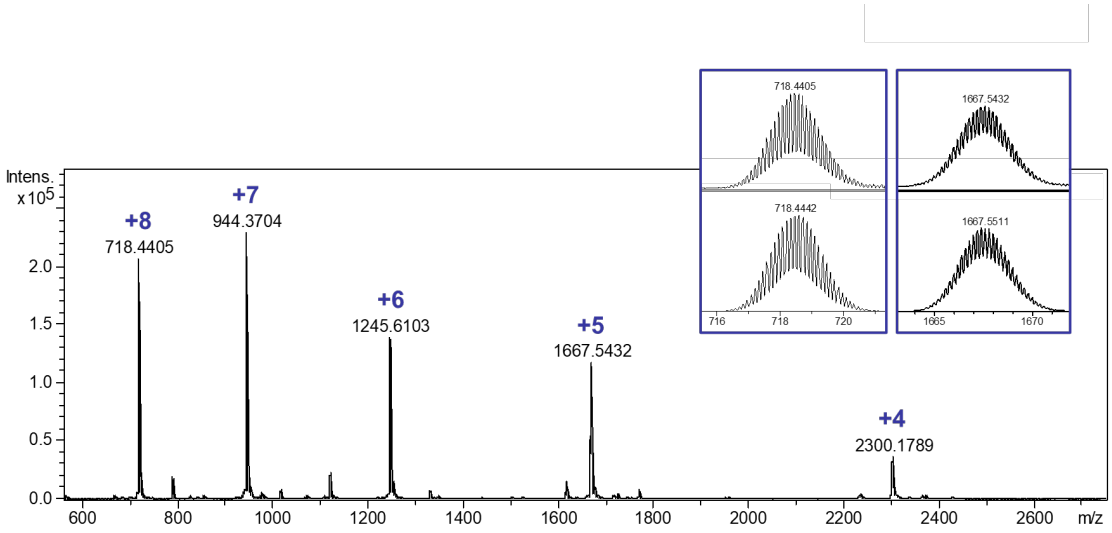

Supplementary Figure 70. HRMS spectrum of **8**·$(BArF)_8$ nanocapsule. Experimental (top) and theoretical (bottom) isotopic pattern for selected peaks is shown. The sample was dissolved in acetonitrile and the spectrum was registered on a Bruker Micro TOF-Q-II exact mass spectrometer.

2.8. Characterization of tetragonal prismatic nanocapsule 9·(BArF)$_8$

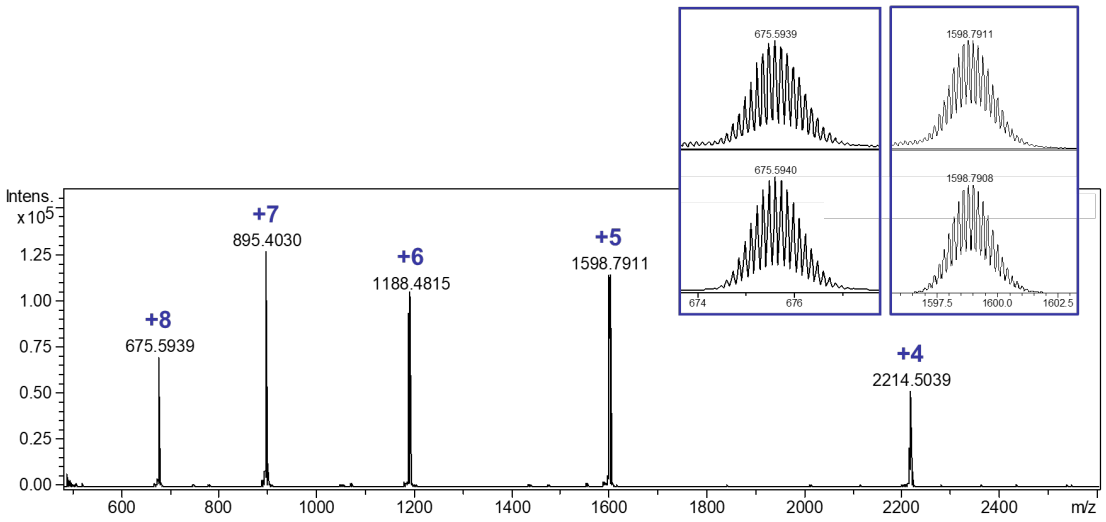

Supplementary Figure 71. HRMS spectrum of **9**·(BArF)$_8$ nanocapsule. Experimental (top) and theoretical (bottom) isotopic pattern for selected peaks is shown. The sample was dissolved in acetonitrile and the spectrum was registered on a Bruker Micro TOF-Q-II exact mass spectrometer.

3. Supplementary References

1. C. García-Simón, C. Colomban, Y. A. Çetin, A. Gimeno, M. Pujals, E. Ubasart, C. Fuertes-Espinosa, K. Asad, N. Chronakis, M. Costas, J. Jiménez-Barbero, F. Feixas and X. Ribas, *J. Am. Chem. Soc.*, 2020, **142**, 16051-16063.
2. J. C. Hummelen, B. Knight, J. Pavlovich, R. González and F. Wudl, *Science*, 1995, **269**, 1554-1556.
3. E. Ubasart, O. Borodin, C. Fuertes-Espinosa, Y. Xu, C. García-Simón, L. Gómez, J. Juanhuix, F. Gándara, I. Imaz, D. Maspoch, M. von Delius and X. Ribas, *Nat. Chem.*, 2021, **13**, 420-427.
4. O. Prakash, H. Joshi, K. N. Sharma, A. K. Sharma and A. K. Singh, *Eur. J. Inorg. Chem.*, 2015, **2015**, 520-526.
5. D. Brynn Hibbert and P. Thordarson, *Chem. Commun.*, 2016, **52**, 12792-12805.